Supporting Information

Penicimutamides A–C: Rare Carbamate-containing Alkaloids from a Mutant of the Marine-derived *Penicillium purpurogenum* G59

Chang-Wei Li,[a,‡] Chang-Jing Wu,[a,‡] Cheng-Bin Cui,[a,*] Lan-Lan Xu,[b] Fei Cao[b] and Hua-Jie Zhu[b]

[a] *State Key Laboratory of Toxicology and Medical Countermeasures, Beijing Institute of Pharmacology and Toxicology, Beijing 100850, China*

[b] *Chinese Center for Chirality, Key Laboratory of Medicinal Chemistry and Molecular Diagnostics of the Ministry of Education, College of Pharmacy, Hebei University, Baoding 071002, Hebei, China*

‡ These authors contributed equally to this work.

* To whom correspondence should be addressed. Email: cuicb@126.com or cuicb@sohu.com; Fax & Tel: 86-10-68211656.

Table of Contents

Experimental Section

General Experimental Procedures. Melting points were measured on a Beijing Tiandiyu X-4 exact micro melting point apparatus (Tiandiyu science and technology Co., Ltd, Beijing, China) and the temperatures were not corrected. Optical rotations were recorded on an Optical Activity Limited PolAAr 3005 spectropolarimeter (Optical Activity Limited, Ramsey, United Kingdom). ESIMS and HRESIMS were measured on AB SCIEX Applied Biosystems API 3000 LC-MS (AB SCIEX, Framingham, USA) and Agilent 6520 Q-TOF LC-MS spectrometers (Agilent Technologies, Santa Clara, CA, USA), respectively. UV and IR spectra were recorded on GBC Cintra 20 spectrophotometer (GBC, Melbourne, Australia) and Bruker Tensor-27 infrared spectrophotometers (Bruker, Karlsruhe, Germany), respectively. CD data were measured on a Bio-Logic Science MOS450 CD spectrometer (Bio-Logic, Pont-de-Claix, France). NMR spectra were acquired on a Bruker-600 (600 MHz for ^{1}H/150 MHz for ^{13}C) NMR spectrometer (Bruker, Karlsruhe, Germany). X-ray crystallography analysis was carried out on an Agilent Gemini E Ultra CCD diffractometer (Agilent Technologies, Santa Clara, CA, USA) with graphite-monochromated Cu Kα radiation (λ = 1.54178 Å). TLC was performed using pre-coated silica gel GF_{254} plates (0.25-mm thickness, Yantai Chemical Industrial Institute, Yantai, China). The TLC spots were detected under sunlight and UV light (254 and 365 nm) illumination or using Vaughan's reagent.[1] Column chromatography was performed using Silica gel H (200–300 mesh, Yantai Chemical Industrial Institute), YMC*GEL® ODS-A-HG (12 nm S-50 μm, YMC Co., Ltd, Kyoto, Japan), or Sephadex™ LH-20 (GE Healthcare, Uppsala, Sweden). HPLC was performed on a Waters HPLC system equipped with a Waters 600 controller, a Waters 600 pump, a Waters 2414 refractive index detector and a Waters 2996 (for analytical HPLC) or 2998 (for preparative HPLC) photodiode array detector using Waters Empower™ software (Waters, Milford, MA, USA). Venusil MP C_{18} (5 μm, 100 Å, 4.6 × 250 mm; Agela Technologies, Tianjin, China) and Capcell Pak C_{18} (MG II, 4.6 × 250 mm; Shiseido Co., Ltd, Tokyo, Japan) columns were used for analytical HPLC. A Capcell Pak C_{18} (MG II, 20 × 250 mm; Shiseido Co., Ltd, Tokyo, Japan) column was used for preparative HPLC. Cell morphology was examined using an AE31 EF-INV inverted microscope (Motic China Group Co., Ltd, Xiamen, Fujian, China). Optical density (OD) was measured on a VersaMax-BN03152 micro plate reader (Molecular Devices, Silicon Valley, CA, USA). ZHWY-2102 rotary shakers (Shanghai ZhiCheng Analyzing Instrument Manufactory Co., Ltd, Shanghai, China) were used for the fermentation processes.

Cell Lines and Reagents. Human chronic myelogenous leukemia K562 cells were provided by Li-Li Wang (Beijing Institute of Pharmacology and Toxicology, Beijing, China). Human cancer cells, acute promyelocytic leukemia HL-60, cervical cancer HeLa and gastric adenocarcinoma BGC-823, were provided by Wen-Xia Zhou (Beijing Institute of Pharmacology and Toxicology). Fetal bovine serum was purchased from Tianjin Hao Yang Biological Manufacture Co., Ltd (Tianjin, China). RPMI-1640 medium (lot no. 1403238) and MTT (lot no. 0793) were purchased from Gibco (Grant Island, NY, USA) and Amresco (Solon, OH, USA), respectively. Streptomycin (lot no. 071104) and penicillin (lot no. X11303302) were purchased from North China Pharmaceutical

Group Corporation (Beijing, China). 5-Fluorouracil (5-FU, lot no. 5402) was purchased from Aladdin Chemistry Co., Ltd (Shanghai, China).

Fungal Strains. The parent fungal G59 strain was isolated from a soil sample collected at the tideland of Bohai Bay around Lüjühe in the Tanggu district of Tianjin, China, in September 2004.[2] This strain was identified as *Penicillium purpurogenum* G59 by Liang-Dong Guo of the Institute of Microbiology of the Chinese Academy of Sciences, Beijing, China. This strain has been deposited at the China General Microbiological Culture Collection Center (CGMCCC) under the accession number CGMCC No. 9721. AD-2-1 is a bioactive mutant from the diethyl sulfate (DES) mutagenesis of *P. purpurogenum* G59. This mutant was selected by our group in a previous study by the treatment of fresh G59 spores with 1% (v/v) DES in 50% (v/v) DMSO at 4 °C for 1 day.[3] This mutant strain has been deposited at the CGMCCC under the accession number CGMCC No. 3561.

Fermentation and Extraction. Spore suspensions of the mutant AD-2-1 and parent G59 strains were prepared using fresh spores according to a previously reported procedure.[4] The spore density of the suspensions was adjusted to a OD value of 0.35 by monitoring the OD at 600 nm, which was measured on a VersaMax-BN03152 micro plate reader.

The fermentation of the mutant AD-2-1 was conducted in thirty 500-mL Erlenmeyer flasks, each containing 50 g of rice. Distilled water (80 mL) was added to each flask, and the contents were soaked overnight before autoclaving at 121 °C for 30 min. After cooling to room temperature, an aliquot (1 mL) of the AD-2-1 spore suspension was inoculated into each flask, and the flasks were incubated at 28 °C for 50 days. The fermented material in each flask was extracted with 300 mL of ethyl acetate (EtOAc) under ultrasonic irradiation for 2 h to afford an EtOAc solution, which was carefully poured out the container after being left to stand for a period of time. The remaining solid substances in each flask were further extracted with EtOAc (2 × 300 mL) in the same manner. The EtOAc solutions were combined and evaporated to dryness to obtain an EtOAc extract (75.2 g), which was suspended in 500 mL of MeOH. The MeOH suspension was agitated under ultrasonic irradiation to aid the dissolution of the MeOH-soluble materials in the mixture. The insoluble part was removed by filtration (12.5 g, mainly the mycelial components), and the filtrate was extracted with 500 mL petroleum ether (b.p. 60–90 ºC) to remove a lipophilic fraction (25.2 g). This fraction was later analyzed by HPLC to confirm that it did not contain **1**–**3**. The remaining MeOH layer was evaporated to dryness to give a MeOH extract (27.5 g). This MeOH extract inhibited K562 cells with an inhibition rate (IR%) of 62.5% at 100 μg/mL. Compounds **1**–**3** were isolated from this extract. The parent G59 strain was fermented and extracted in the same manner. One 500-mL Erlenmeyer flask was used to obtain a MeOH extract (0.92 g). Notably, this extract did not exhibit any inhibitory effect on K562 cells (an IR% of 6.1% at 100 μg/mL). This G59 extract was consequently used as the negative control in the separation of the mutant AD-2-1 extract for tracking the production of **1**–**3** by this mutant strain. The MeOH extracts of the mutant AD-2-1 and parent G59 strains were used in the HPLC-photo diode array detector (PDAD)-UV and HPLC- ESI-MS analyses to detect **1**–**3**.

Isolation of Compounds 1–3. The MeOH extract (27.4 g) of the mutant AD-2-1 was fractionated by vacuum liquid chromatography (VLC) on a silica gel column (silica gel 80 g, bed 6.6 × 15.0 cm). A stepwise elution of the column with b.p. 60–90 ºC petroleum ether (P)–dichloromethane (D)–

MeOH (M) afforded ten fractions: **Fr-1** (1.1 g, eluted by P), **Fr-2** (2.1 g, eluted by PD 1:1), **Fr-3** (2.5 g, eluted by PD 1:5 → D), **Fr-4** (3.2 g, eluted by DM 99:1), **Fr-5** (2.1 g, eluted by DM 98:2 → 97:3), **Fr-6** (5.2 g, eluted by DM 97:3 → 95:5), **Fr-7** (3.5 g, eluted by DM 95:5 → 92:8), **Fr-8** (3.5 g, eluted by DM 92:8 → 90:10), **Fr-9** (2.1 g, eluted by DM 90:10 → 80:20) and **Fr-10** (0.9 g, eluted by DM 80:20 → 70:30). **Fr-6** (5.2 g) was subjected to VLC on an ODS column (ODS 50 g, bed 5.0 × 8.0 cm) eluted with M–H_2O (W) (20:80 → 100:0) to obtain four fractions: **Fr-6-1** (1.7 g, eluted by MW 20:80), **Fr-6-2** (1.9 g, eluted by MW 20:80 → 50:50), **Fr-6-3** (0.65 g, eluted by MW 50:50 → 80:20) and **Fr-6-4** (0.8 g, eluted by MW 80:20 → 100:0). **Fr-6-2** (1.9 g) was further separated over a Sephadex LH-20 column (bed 4.8 × 42 cm) eluting with 95% ethanol to afford four fractions: **Fr-6-2-1** (270 mg), **Fr-6-2-2** (420 mg), **Fr-6-2-3** (960 mg) and **Fr-6-2-4** (160 mg). **Fr-6-2-1** (270 mg) was subjected to preparative HPLC (column, Capcell Pak C_{18}, MG II, 20 × 250 mm, temperature, 26 °C; mobile phase, 64% MeOH; flow rate, 6.0 mL/min; detection wavelengths, 210 and 270 nm) to obtain crude samples of **1** (16 mg, t_R = 13.5–17.0 min), **2** (23 mg, t_R = 44.0–50.0 min) and **3** (30 mg, t_R = 28.5–33.5 min). These crude samples of **1**–**3** were purified by HPLC under the same conditions to afford **1** (12 mg), **2** (18 mg) and **3** (21 mg).

Penicimutamide A (1): colorless needles (MeOH), m.p. 168–170 °C, $[\alpha]_D^{20}$ −35.4 (*c* 0.71, MeOH). Positive ESI-MS *m/z*: 366 $[M + H]^+$, 388 $[M + Na]^+$, 731 $[2M + H]^+$, 753 $[2M + Na]^+$; negative ESI-MS *m/z*: 364 $[M - H]^-$, 400 $[M + Cl]^-$, 410 $[M + HCOO]^-$, 729 $[2M - H]^-$. HR-ESI-MS *m/z*: measured 366.1814 $[M + H]^+$, calcd for $C_{21}H_{24}N_3O_3$ $[M + H]^+$ 366.1818; measured 388.1616 $[M + Na]^+$, calcd for $C_{21}H_{23}N_3O_3Na$ $[M + Na]^+$ 388.1637; measured 404.1384 $[M + K]^+$, calcd for $C_{21}H_{23}N_3O_3K$ $[M + K]^+$ 404.1376. UV λ_{max} (log ε) in MeOH: 219 (4.36), 265 (3.50). IR ν_{max} cm^{-1} (diamond ATR crystal): 3257, 3129, 2969, 2933, 2866, 1717, 1623, 1582, 1458, 1354, 1334, 1318, 1117, 1085, 1061, 1008, 778, 744 cm^{-1}. CD $\Delta\varepsilon$ (nm) in MeOH: –5.54 (200), –6.06 (224.5), 0 (236), +5.20 (256), 0 (273), –1.16 (280), 0 (287.5), +1.59 (298.5), 0 (326). ^1H and ^{13}C NMR data: Tables S1 and S2.

X-ray Data of (1): $C_{21}H_{23}N_3O_3$, M = 365.42, orthorhombic, a = 11.3978(10) Å, b = 14.6540(12) Å, c = 21.3097(19) Å, U = 3559.2(5) $Å^3$, T = 99.8, space group $P2_12_12_1$ (no. 19), Z = 8, μ(Cu Kα) = 0.749. Of the 26574 reflections that were collected, 6072 were unique (R_{int} = 0.0823). The structure of **1** was solved by direct methods using SHELXL-97 and refined by full-matrix least-squares on F^2. Final refinement: data/restraints/parameters = 6072/0/491; R_1 = 0.0584 (all data), wR_2 = 0.1346 (all data). The crystallographic data (including structure factors) reported in this paper for **1** (CCDC 1480828) have been deposited with the Cambridge Crystallographic Data Center (CCDC). Copies of these data can be obtained, free of charge, on application to CCDC, 12 Union Road, CB2 1EZ, UK (Fax: +44-0-1223-336033 or e-mail: deposit@ccdc.cam.ac.uk).

Penicimutamide B (2): a white crystalline powder (MeOH), m.p. 164–166 °C, $[\alpha]_D^{20}$ +18.8 (*c* 0.6, MeOH). Positive ESI-MS *m/z*: 350 $[M - OH]^+$, 368 $[M + H]^+$, 382 $[M - OH + CH_3OH]^+$, 404 $[M - H_2O + CH_3OH + Na]^+$; negative ESI-MS *m/z*: 367 $[M]^-$, 402 $[M + Cl]^-$, 426 $[M + CH_3CO_2]^-$, 769 $[2M + Cl]^-$. HR-ESI-MS *m/z*: measured 350.1860 $[M - OH]^+$, calcd for $C_{21}H_{24}N_3O_2$ $[M - OH]^+$ 350.1869; measured 368.1966 $[M + H]^+$, calcd for $C_{21}H_{26}N_3O_3$ $[M + H]^+$ 3368.1974; measured

382.2123 [M – OH + CH_3OH]$^+$, calcd for $C_{22}H_{28}N_3O_3$ [M – OH + CH_3OH]$^+$ 382.2131; measured 404.1939 [M – H_2O + CH_3OH + Na]$^+$, calcd for $C_{22}H_{27}N_3O_3Na$ [M – H_2O + CH_3OH + Na]$^+$ 404.1950. UV λ_{max} (log ε) in MeOH: 220 (4.34), 264 (3.56). IR ν_{max} cm^{-1} (diamond ATR crystal): 3401, 2970, 2940, 2874, 1705, 1580, 1459, 1367, 1320, 1282, 1216, 1171, 1128, 1088, 1045, 1025, 755, 732. CD $\Delta\varepsilon$ (nm) in MeOH: –2.91 (200), –11.43 (223.5), 0 (235), +6.34 (256.5), 0 (273.5), –1.02 (278.5), 0 (286), +1.56 (298), 0 (314.5). ^{1}H and ^{13}C NMR data: Tables S3 and S4.

Penicimutamide C (3): a white wax (MeOH), $[\alpha]_D^{20}$ –66.7 (*c* 1.73, MeOH). Positive ESI-MS *m/z*: 352 [M + H]$^+$, 374 [M + Na]$^+$, 390 [M +K]$^+$, 703 [2M + H]$^+$, 725 [2M + Na]$^+$; negative ESI-MS *m/z*: 350 [M – H]$^–$. HR-ESI-MS *m/z*: measured 352.2043 [M + H]$^+$, calcd for $C_{21}H_{26}N_3O_2$ [M + H]$^+$ 352.2025; measured 374.1842 [M + Na]$^+$, calcd for $C_{21}H_{25}N_3O_2Na$ [M + Na]$^+$ 374.1844; measured 390.1582 [M + K]$^+$, calcd for $C_{21}H_{25}N_3O_2K$ [M + K]$^+$ 390.1584; measured 703.3967 [2M + H]$^+$, calcd for $C_{42}H_{51}N_6O_4$ [2M + H]$^+$ 703.3972; measured 725.3792 [2M + Na]$^+$, calcd for $C_{42}H_{50}N_6O_4Na$ [2M + Na]$^+$ 725.3791. UV λ_{max} (log ε) in MeOH: 220 (4.39), 264 (3.64). IR ν_{max} cm^{-1} (diamond ATR crystal): 3385, 3287, 2935, 2858, 2794, 1722, 1579, 1459, 1416, 1320, 1303, 1087, 1028, 1012, 768, 754, 731. CD $\Delta\varepsilon$ (nm) in MeOH: –5.10 (200), –8.49 (225), 0 (235.5), +6.96 (255.5), 0 (273), –1.39 (279.5), 0 (287.5), +1.66 (298.5), 0 (317). ^{1}H and ^{13}C NMR data: Tables S5 and S6.

HPLC-PDAD-UV and HPLC-ESI-MS Analysis. The MeOH extracts of the mutant AD-2-1 and parent G59 strains were dissolved in MeOH to prepare sample solutions at 10 mg/mL for HPLC-PDAD-UV and HPLC-ESI-MS analyses. Solutions of **1**–**3** in MeOH at 10 mg/mL were used as the reference standards for the HPLC-PDAD-UV analysis. HPLC-PDAD-UV analysis was performed on a Venusil MP C_{18} column (5 μm, 100 Å, 4.6 × 250 mm, temperature, 25 °C) using the Waters HPLC system described above in the General Experimental Procedures. The sample and standard solutions were filtered through a 0.22 μm membrane filter prior to being used. A sample volume of 5 μL was injected onto the column. The elution was performed using a linear gradient of MeOH–H_2O (20% MeOH at 0 min → 100% MeOH at 60 min → 100% MeOH at 90 min; flow rate, 1.0 mL/min). The acquired photodiode array data were processed using the Waters Empower™ software to obtain the targeted HPLC-PDAD-UV data. The retention times (t_R) of **1**–**3** were 35.9, 51.1 and 48.3 min, respectively. Compounds **1**–**3** were detected in the mutant AD-2-1 extract based on their t_R and UV spectra. However, all they were not detected in the parent G59 extract. HPLC-ESI-MS analysis was performed on a LC-MS equipment equipped with an Agilent 1100 HPLC system and an AB Sciex API 3000 LC-MS/MS system using the AB Sciex Analyst 1.4 software (AB SCIEX, Framingham, MA, USA). HPLC analysis was conducted on the same Venusil MP C_{18} column (5 μm, 100 Å, 4.6 × 250 mm) under identical conditions to the HPLC-PDAD-UV analysis. The mass detector was set to scan *m/z* values in the range of 150 to 1,500 in both the positive and negative ionization modes. The acquired data were processed using the Analyst 1.4 software to obtain the targeted HPLC-ESI-MS data. The *pseudo*-molecular ions of **1**–**3** appeared as peaks with t_R values of 30.46, 46.28 and 42.07 min, respectively, in the positive ionization mode. The retention times were slightly shorter than in the HPLC-PDAD-UV analysis because of the shorter flow length from the outlet of the HPLC column to the inlet of the MS in the HPLC-ESI-MS system. Compounds **1**–**3** were also only detected

in the mutant extract, with no evidence of these compounds in the parent G59 extract by selective ion monitoring (*m*/*z*: 388 $[M + Na]^+$ for **1**, 368 $[M + H]^+$ for **2** and 352 $[M + H]^+$ for **3**) of the extracted ion chromatograms and the related MS data.

Computational Section. All of quantum chemical calculations were conducted using the Gaussian 09 software package.[5] In TDDFT ECD calculations, conformational searches were performed at the molecular mechanics level using the MMFF94S force field incorporated in Hyperchem 7.0 for **1**, ***ent*-1**, **2**, ***ent*-2**, **3**, ***ent*-3**, **4** and **4a**. Two conformations (0–10 kcal/mol) were found for each of these compounds. All of these conformations were re-optimized at the B3LYP/6-31–G(d) level in the gas phase. There were two B3LYP/6-31–G(d)-optimized conformers (0–4.6 kcal/mol) for each absolute configuration, one of which possessed the 99% Boltzmann population. The conformers were further optimized at the B3LYP/6-311+G(d) level in the gas phase, and one B3LYP/6-311+G(d)-optimized conformer (99% Boltzmann population) was used for the ECD computation at the CAM-B3LYP/6-311++G(2d,p) level in the gas phase. ECD spectra were simulated using the velocity strength data with a standard deviation of 0.35 eV. The calculated spectrum was then compared with the measured data. In the specific optical rotation ($[\alpha]_D$) calculations for **4**, the lowest-energy conformer from the conformational searches of **4** was further geometry-optimized at the B3LYP/6-311++G(2d,p), PCM (MeOH)/B3LYP/6-311++G(2d,p), IEFPCM(MeOH)/B3LYP/6-311++G(2d,p) and SMD(MeOH)/B3 LYP/6-311++G(2d,p) level, respectively. The $[\alpha]_D$ calculation was performed at first at the B3LYP/ 6-311++G(2d,p) level using the optimized B3LYP/6-311++G(2d,p) in gas phase and PCM(MeOH)/ B3LYP/6-311++G(2d,p) in MeOH geometries, which afforded the $[\alpha]_D$ values of +78.5 and +71.5, respectively. Then, further $[\alpha]_D$ calculations were performed at the IEFPCM (MeOH)/B3LYP/6-311++G(2d,p) level using the optimized IEF PCM(MeOH)/B3LYP/6-311++G (2d,p) in MeOH geometry and at the SMD(MeOH)/B3LYP/6-311++G(2d,p) level using the optimized SMD(MeOH)/ B3LYP/6-311++G(2d,p) in MeOH geometry, respectively. The former and the latter calculations afforded the $[\alpha]_D$ values of +32.0 and +15.5, respectively.

MTT Assay. The MTT assay was performed according to a previously reported procedure.[1–4] Exponentially growing K562, HL-60, HeLa and BGC-823 cells were treated with samples at 37 °C for 24 h. Assay was performed in triplicate, and the OD was determined at 570 nm on a VersaMax-BN03152 plate reader. The IR% was calculated using the mean value of the OD according to the formula: $IR\% = (OD_{control} - OD_{sample})/OD_{control} \times 100\%$. The IC_{50} for **2** was determined based on its IR% values at different concentrations. The MeOH extracts and **1**−**3** in MeOH at 10.0 mg/mL, 5-FU in 20% (v/v) aqueous DMSO at 10.0 mg/mL and serial dilutions of the MeOH solution of **2** at 10.0 mg/mL were used in the MTT assay. 5-FU was used as a positive control. MeOH and the 20% (v/v) aqueous DMSO solution were used as blank controls.

References

1. (a) C.-J. Wu, C.-W. Li and C.-B. Cui, *Mar. Drugs*, 2014, **12**, 1815. (b) M.-W. Xia, C.-B. Cui, C.-W. Li and C.-J Wu, *Mar. Drugs*, 2014, **12**, 1545.
2. C.-K. Tian, C.-B. Cui and X.-X. Han, *J. Int. Pharm. Res.,* 2008, **35**, 401.
3. S.-M. Fang, C.-J.Wu, C.-W. Li and C.-B. Cui, *Mar. Drugs*, **2014**, *12*, 1788.
4. (a) Y.-J. Chai, C.-B. Cui, C.-W. Li, C.-J. Wu, C.-K. Tian and W. Hua, *Mar. Drugs*, 2012, **10**, 559. (b) S.-M. Fang, C.-B. Cui, C.-W. Li, C.-J. Wu, Z.-J. Zhang, L. Li, X.-J. Huang and W.-C. Ye, *Mar. Drugs*, 2012, **10**, 1266.
5. *Gaussian 09*, Revision A.01; Gaussian Inc.: Wallingford, CT, USA, 2009.

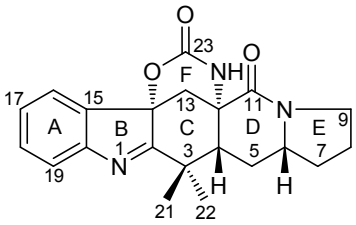

Penicimutamide A (**1**)

Table S1. 600 MHz ^{1}H and 150 MHz ^{13}C NMR data of **1** in CD_3OD.[a]

No.	δ_C [b,c]	δ_H (*J* in Hz) [b]	COSY [d]	HMBC [e]	NOE [f]
2	187.4 s	—	—	—	—
3	40.6 s	—	—	—	—
4	52.4 d	2.04 dd (13.0, 1.8)	H_2-5	C-3,5,6,12,13,21,22	Hβ-5,13, H-6, H_3-21
5	25.7 t	Hα 1.73 td (13.0, 11.6)	H-4, Hβ-5, H-6	C-4,6,7,12	Hβ-5, Hα-7, H_3-22
		Hβ 2.23 ddd (13.0, 4.6, 1.8)	H-4, Hα-5, H-6	C-3,4,6,12	Hα-5, H-4,6, H_3-21,22
6	61.6 d	3.53 tt (11.6, 4.6)	H_2-5, H_2-7	C-4,5,7,8,11	H-4, Hβ-5,7,8
7	33.5 t	Hα 1.65 qd (11.6, 7.8)	H-6, Hβ-7, H_2-8	C-5,6,8	Hα-5,8, Hβ-7
		Hβ 2.19–2.14 m	H-6, Hα-7, H_2-8	C-8,9	H-6, Hα-7, Hβ-8
8	23.2 t	Hα 2.09–2.02 m	H_2-7, Hβ-8, H_2-9	C-6,7	Hα-7,9, Hβ-8
		Hβ 1.93–1.83 m	H_2-7, Hα-8, H_2-9	C-7,9	Hβ-7,9, Hα-8
9	46.6 t	Hα 3.63 dt (12.2, 9.0)	H_2-8, Hβ-9	C-6,8,11	Hα-8, Hβ-9
		Hβ 3.39 ddd (12.2, 9.8, 1.9)	H_2-8, Hα-9	C-7,8	Hβ-8, Hα-9
11	167.4 s	—	—	—	—
12	58.2 s	—	—	—	—
13	36.9 t	Hα 3.17 d (13.8)	Hβ-13	C-2,4,5,11,12,14,15	Hβ-13, H-16
		Hβ 1.87 d (13.8)	Hα-13	C-2,4,11,12,14,15	H-4, Hα-13
14	88.0 s	—	—	—	—
15	137.3 s	—	—	—	—
16	124.4 d	7.56 br d (7.8)	H-17, 18	C-14,18,20	Hα-13, H-17
17	128.2 d	7.34 td (7.8, 1.2)	H-16, 18, 19	C-15,19	H-16,17
18	132.0 d	7.47 td (7.8, 1.2)	H-16, 17, 19	C-16,20	H-17,19
19	121.7 d	7.52 br d (7.8)	H-17, 18	C-15,17	H-18
20	153.9 s	—	—	—	—
21	27.7 q	1.50 3H, s	H_3-22	C-2,3,4,22	H-4, H_3-22, Hβ-5
22	21.6 q	1.28 3H, s	H_3-21	C-2,3,4,21	H_2-5, H_3-21
23	155.1 s	—	—	—	—

[a] Signals assignments were based on the results of DEPT, ^{1}H-^{1}H COSY, HMQC, and HMBC experiments. [b] Chemical shift values (δ_H and δ_C) were recorded using the solvent signals (CD_3OD: δ_H 3.31/δ_C 49.00) as references, respectively. [c] Multiplicities of the carbon signals were determined by DEPT experiments and are indicated as s (singlet), d (doublet), t (triplet) and q (quartet), respectively. [d] The numbers in each line of this column indicate the protons that correlated with the proton in the corresponding line in ^{1}H-^{1}H COSY. [e] The numbers in each line of this column indicate the carbons that showed HMBC correlations with the proton in the corresponding line in the HMBC experiments optimized for the 8.3 Hz of long-range J_{CH} value. [f] Numbers in each line of this column indicate the protons that showed NOE correlations with the proton in the corresponding line in NOESY experiment.

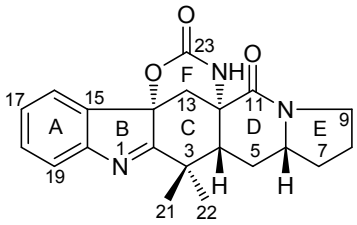

Penicimutamide A (**1**)

Table S2. 600 MHz ^{1}H and 150 MHz ^{13}C NMR data of **1** in acetone-d_6.[a]

No.	δ_C [b,c]	δ_H (J in Hz) [b]	COSY [d]	HMBC [e]	NOE [f]
2	186.9 s	—	—	—	—
3	40.1 s	—	—	—	—
4	52.0 d	2.05 m (overlapped)	H_2-5	C-3,5,6,12,13,21,22	Hβ-5,13, H-6, H_3-21
5	25.7 t	Hα 1.90 td (12.8, 11.5)	H-4, Hβ-5, H-6	C-4,6,7,12,13	Hβ-5,Hα-7,H_3-22,N<u>H</u>
		Hβ 2.25 ddd (12.8, 4.0, 1.6)	H-4, Hα-5, H-6	C-3,4,6,7,12	Hα-5, H-4,6,H_3-21,22
6	60.6 d	3.56–3.48 m	H_2-5, H_2-7	C-4,5,7,8,11	H-4, Hβ-5,7
7	33.3 t	Hα 1.68 qd (11.6, 7.6)	H-6, Hβ-7, H_2-8	C-5,6,8	Hα-5,8, Hβ-7
		Hβ 2.13 dt (11.6, 5.8)	H-6, Hα-7, H_2-8	C-8,9	H-6, Hα-7, Hβ-8
8	22.9 t	Hα 2.02–1.95 m	H_2-7, Hβ-8, H_2-9	C-6,7	Hα-7,9, Hβ-8
		Hβ 1.86–1.79 m	H_2-7, Hα-8, H_2-9	C-7,9	Hβ-7,9, Hα-8
9	45.9 t	Hα 3.56–3.48 m	H_2-8, Hβ-9	C-6,7,8,11	Hα-8, Hβ-9
		Hβ 3.28 ddd (12.2, 9.8, 2.2)	H_2-8, Hα-9	C-7,8	Hβ-8, Hα-9
11	165.9 s	—	—	—	—
12	57.7 s	—	—	—	—
13	36.9 t	Hα 3.18 d (13.9)	Hβ-13	C-2,4,5,11,12,14,15	Hβ-13, H-16
		Hβ 1.80 d (13.9)	Hα-13	C-4,5,11,12,15	H-4, Hα-13
14	87.3 s	—	—	—	—
15	137.9 s	—	—	—	—
16	124.2 d	7.63 br d (7.5)	H-17, 18	C-14,17,18,19,20	Hα-13, H-17
17	127.3 d	7.32 td (7.5, 1.0)	H-16, 18	C-15,16,18,19,20	H-16,17
18	131.3 d	7.45 td (7.5, 1.2)	H-16, 17, 19	C-15,16,17,20	H-17,19
19	121.5 d	7.50 br d (7.5)	H-17, 18	C-15,17,18,20	H-18
20	154.2 s	—	—	—	—
21	27.8 q	1.48 3H, s	H_3-22	C-2,3,4,22	H-4, H_3-22, Hβ-5
22	21.7 q	1.28 3H, s	H_3-21	C-2,3,4,21	H_2-5, H_3-21, N<u>H</u>
23	152.4 s	—	—	—	—
N<u>H</u>		7.49 br s	—	—	Hα-5, H_3-22

[a] Signals assignments were based on the results of DEPT, ^{1}H-^{1}H COSY, HMQC, and HMBC experiments. [b] Chemical shift values (δ_H and δ_C) were recorded using the solvent signals (CD_3COCD_3: δ_H 2.05/δ_C 29.84) as references, respectively. [c] Multiplicities of the carbon signals were determined by DEPT experiments and are indicated as s (singlet), d (doublet), t (triplet) and q (quartet), respectively. [d] The numbers in each line of this column indicate the protons that correlated with the proton in the corresponding line in ^{1}H-^{1}H COSY. [e] The numbers in each line of this column indicate the carbons that showed HMBC correlations with the proton in the corresponding line in the HMBC experiments optimized for the 8.3 Hz of long-range J_{CH} value. [f] Numbers in each line of this column indicate the protons that showed NOE correlations with the proton in the corresponding line in NOESY and 1D GOESY NOE experiment.

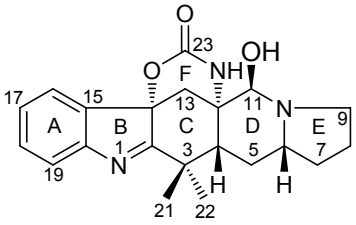

Penicimutamide B (**2**)

Table S3. 600 MHz ^{1}H and 150 MHz ^{13}C NMR data of **2** in CD_3OD.[a]

No.	δ_C [b,c]	δ_H (*J* in Hz) [b]	COSY [d]	HMBC [e]	NOE [f]
2	188.5 s	—	—	—	—
3	40.2 s	—	—	—	—
4	48.4 d	1.97–1.85 m	H_2-5	C-3,5,6,12,13,21,22	Hβ-5,13, H-6, H_3-21
5	28.9 t	Hα 1.52–1.40 m	H-4, Ha-5, H-6	C-4,6,7,12	Hβ-5, Hα-7, H_3-22
		Hβ 1.97–1.85 m	H-4, Hb-5, H-6	C-3,4,12	Hα-5, H-4,6, H_3-21,22
6	55.2 d	2.80–2.73 m	H_2-5, H_2-7	C-4	H-4, Hβ-5,7, Hβ-9
7	31.4 t	Hα 1.52–1.40 m	H-6, Hβ-7, H_2-8	C-5,6,8	Hα-5,8, Hβ-7
		Hβ 1.97–1.85 m	H-6, Hα-7, H_2-8	C-6,9	H-6, Hα-7, Hβ-8
8	22.8 t	Hα 1.97–1.85 m	H_2-7, Hβ-8, H_2-9	C-6,7	Hα-7,9, Hβ-8
		Hβ 1.79–1.72 m	H_2-7, Hα-8, H_2-9	C-7	Hβ-7,9, Hα-8
9	49.3 t	Hα 3.06 td (8.4, 3.0)	H_2-8, Hβ-9	C-6,7,8	Hα-8, Hβ-9, H-11
		Hβ 2.87 q (8.4)	H_2-8, Hα-9	C-8,11	H-6, Hβ-8, Hα-9, H-11
10	—	—	—	—	—
11	95.1 d	4.09 s	—	C-4,6,12,13	H_2-9, Hα-13
12	57.6 s	—	—	—	—
13	37.8 t	Hα 2.57 d (13.8)	Hβ-13	C-2,4,5,11,12,14,15	Hβ-13, H-11,16
		Hβ 1.88 d (13.8)	Hα-13	C-4,11,12,14,15	H-4, Hα-13
14	88.3 s	—	—	—	—
15	137.5 s	—	—	—	—
16	124.3 d	7.53 br d (7.8)	H-17, 18	C-14,18,20	Hα-13, H-17
17	127.9 d	7.32 td (7.8, 1.2)	H-16, 18, 19	C-15,19	H-16,17
18	131.8 d	7.46 td (7.8, 1.2)	H-16, 17, 19	C-16,20	H-17,19
19	121.6 d	7.52 br d (7.8)	H-17, 18	C-15,17	H-18
20	153.8 s	—	—	—	—
21	27.6 q	1.43 3H, s	H_3-22	C-2,3,4,22	H-4, Hβ-5, H_3-22
22	22.6 q	1.20 3H, s	H_3-21	C-2,3,4,21	H_2-5, H_3-21
23	155.1 s	—	—	—	—

[a] Signals assignments were based on the results of DEPT, ^{1}H-^{1}H COSY, HMQC, and HMBC experiments. [b] Chemical shift values (δ_H and δ_C) were recorded using the solvent signals (CD_3OD: δ_H 3.31/δ_C 49.00) as references, respectively. [c] Multiplicities of the carbon signals were determined by DEPT experiments and are indicated as s (singlet), d (doublet), t (triplet) and q (quartet), respectively. [d] The numbers in each line of this column indicate the protons that correlated with the proton in the corresponding line in ^{1}H-^{1}H COSY. [e] The numbers in each line of this column indicate the carbons that showed HMBC correlations with the proton in the corresponding line in the HMBC experiments optimized for the 8.3 Hz of long-range J_{CH} value. [f] Numbers in each line of this column indicate the protons that showed NOE correlations with the proton in the corresponding line in NOESY experiment.

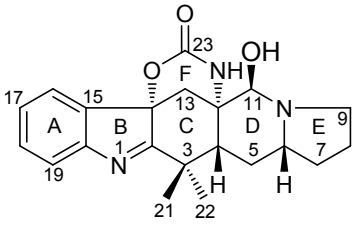

Penicimutamide B (**2**)

Table S4. 600 MHz ^{1}H and 150 MHz ^{13}C NMR data of **2** in acetone-d_6.[a]

No.	δ_C [b,c]	δ_H (J in Hz) [b]	COSY [d]	HMBC [e]	NOE [f]
2	187.8 s	—	—	—	—
3	39.7 s	—	—	—	—
4	47.2 d	1.98 dd (12.7, 3.5)	H_2-5	C-3,5,6,12,13,21,22	Hβ-5,13, H-6, H_3-21,O<u>H</u>
5	28.7 t	Hα 1.54–1.45 m	H-4, Ha-5, H-6	C-3,4,6,7,12	Hβ-5, Hα-7, H_3-22, N<u>H</u>
		Hβ 1.93–1.87 m	H-4, Hb-5, H-6	C-3,4,6,12	Hα-5, H-4,6, H_3-21,22
6	53.9 d	2.84–2.79 m	H_2-5, H_2-7	C-7,11	H-4, Hβ-5,7, Hβ-9, O<u>H</u>
7	31.3 t	Hα 1.54–1.45 m	H-6, Hβ-7, H_2-8	C-5,6,8,9	Hα-5,8, Hβ-7
		Hβ 1.93–1.87 m	H-6, Hα-7, H_2-8	C-6,8,9	H-6, Hα-7, Hβ-8
8	22.3 t	Hα 1.87–1.81 m	H_2-7, Hβ-8, H_2-9	C-6,7,9	Hα-7,9, Hβ-8
		Hβ 1.73–1.65 m	H_2-7, Hα-8, H_2-9	C-7,9	Hβ-7,9, Hα-8
9	47.8 t	Hα 2.89 td (8.6, 3.0)	H_2-8, Hβ-9	C-6,7,8	Hα-8, Hβ-9, H-11
		Hβ 2.83 q (8.4)	H_2-8, Hα-9	C-7,8,11	H-6, Hβ-8, Hα-9, H-11, O<u>H</u>
10	—	—	—	—	—
11	85.0 d	4.44 d (5.1)	O<u>H</u>	C-4,6,12,13	H_2-9, Hα-13, N<u>H</u>, O<u>H</u>
12	56.9 s	—	—	—	—
13	38.4 t	Hα 2.43 d (13.9)	Hβ-13	C-2,4,5,11,12,14,15	Hβ-13, H-11,16
		Hβ 1.89 d (13.9)	Hα-13	C-4,11,12,14,15	H-4, Hα-13, O<u>H</u>
14	87.5 s	—	—	—	—
15	138.1 s	—	—	—	—
16	123.8 d	7.52 br d (7.5)	H-17, 18	C-14,18,19,20	Hα-13, H-17
17	127.1 d	7.28 td (7.5, 1.0)	H-16, 18, 19	C-15,16,18,19,20	H-16,17
18	131.1 d	7.43 td (7.5, 1.2)	H-16, 17, 19	C-15,16,17,20	H-17,19
19	121.6 d	7.50 br d (7.5)	H-17, 18	C-15,16,17	H-18
20	154.3 s	—	—	—	—
21	27.7 q	1.43 3H, s	H_3-22	C-2,3,4,22	H-4, Hβ-5, H_3-22
22	22.6 q	1.20 3H, s	H_3-21	C-2,3,4,21	H_2-5, H_3-21, N<u>H</u>
23	152.2 s	—	—	—	—
N<u>H</u>		6.18 s	—	—	Hα-5, H-11, H_3-22
O<u>H</u>		4.86 d (5.1)	H-11	C-11,12	H-4,6,11, Hβ-9,13

[a] Signals assignments were based on the results of DEPT, ^{1}H-^{1}H COSY, HMQC, and HMBC experiments. [b] Chemical shift values (δ_H and δ_C) were recorded using the solvent signals (CD_3COCD_3: δ_H 2.05/δ_C 29.84) as references, respectively. [c] Multiplicities of the carbon signals were determined by DEPT experiments and are indicated as s (singlet), d (doublet), t (triplet) and q (quartet), respectively. [d] The numbers in each line of this column indicate the protons that correlated with the proton in the corresponding line in ^{1}H-^{1}H COSY. [e] The numbers in each line of this column indicate the carbons that showed HMBC correlations with the proton in the corresponding line in the HMBC experiments optimized for the 8.3 Hz of long-range J_{CH} value. [f] Numbers in each line of this column indicate the protons that showed NOE correlations with the proton in the corresponding line in NOESY and 1D GOESY NOE experiment.

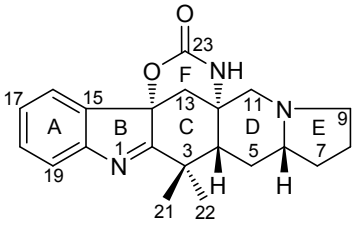

Penicimutamide C (**3**)

Table S5. 600 MHz ^{1}H and 150 MHz ^{13}C NMR data of **3** in CD_3OD.[a]

No.	δ_C [b,c]	δ_H (*J* in Hz) [b]	COSY [d]	HMBC [e]	NOE [f]
2	188.5 s	—	—	—	—
3	40.5 s	—	—	—	—
4	54.16 d	1.61 dd (12.6, 3.3)	H_2-5	C-3,5,6,12,13,21,22	Hβ-5,11,13, H-6, H_3-21
5	28.6 t	Hα 1.51 td (12.6, 10.2)	H-4, Ha-5, H-6	C-4,6,7,12	Hβ-5, Hα-7, H_3-22
		Hβ 2.00–1.92 m	H-4, Hb-5, H-6	C-3,4,6,12	Hα-5, H-4,6, H_3-21,22
6	65.4 d	2.00–1.92 m	H_2-5, H_2-7	C-4,7	H-4, Hβ-5,7,9, Hβ-11
7	31.2 t	Hα 1.59–1.51 m	H-6, Hβ-7, H_2-8	C-5,6,8	Hα-5,8, Hβ-7
		Hβ 2.00–1.92 m	H-6, Hα-7, Hβ-8	C-8,9	H-6, Hα-7, Hβ-8
8	22.5 t	Hα 1.93–1.85 m	Hα-7, Hβ-8, H_2-9	C-6,7,9	Hα-7,9, Hβ-8
		Hβ 1.82–1.76 m	H_2-7, Hα-8, H_2-9	—	Hβ-7,9, Hα-8
9	54.19 t	Hα 3.06 td (9.0, 2.4)	H_2-8, Hβ-9	C-6,7,8	Hα-8,11, Hβ-9
		Hβ 2.17 q (9.0)	H_2-8, Hα-9	C-8,11	H-6, Hβ-8,11, Hα-9
10	—	—	—	—	—
11	62.9 t	Hα 3.02 d (11.4)	—	C-3,4,6,9,13	Hα-9, Hβ-11, Hα-13
		Hβ 2.21 d (11.4)		C-4,6,13	H-4,6, Hα-11, Hβ-9,13
12	54.4 s	—	—	—	—
13	38.8 t	Hα 2.50 d (14.4)	Hβ-13	C-2,4,5,11,12,14,15	Hα-11, Hβ-13, H-16
		Hβ 1.76 d (14.4)	Hα-13	C-4,11,12,15	H-4, Hβ-11, Hα-13
14	88.0 s	—	—	—	—
15	137.4 s	—	—	—	—
16	124.3 d	7.518 br d (7.8)	H-17, 18	C-14,18,20	Hα-13, H-17
17	127.9 d	7.31 td (7.8, 1.2)	H-16, 18, 19	C-15,19	H-16, 17
18	131.8 d	7.45 td (7.8, 1.2)	H-16, 17, 19	C-16,20	H-17, 19
19	121.6 d	7.516 br d (7.8)	H-17, 18	C-15,17	H-18
20	153.9 s	—	—	—	—
21	27.6 q	1.44 3H, s	H_3-22	C-2,3,4,22	H-4, Hβ-5, H_3-22
22	22.2 q	1.22 3H, s	H_3-21	C-2,3,4,21	H_2-5, H_3-21
23	155.0 s	—	—	—	—

[a] Signals assignments were based on the results of DEPT, ^{1}H-^{1}H COSY, HMQC, and HMBC experiments. [b] Chemical shift values (δ_H and δ_C) were recorded using the solvent signals (CD_3OD: δ_H 3.31/δ_C 49.00) as references, respectively. [c] Multiplicities of the carbon signals were determined by DEPT experiments and are indicated as s (singlet), d (doublet), t (triplet) and q (quartet), respectively. [d] The numbers in each line of this column indicate the protons that correlated with the proton in the corresponding line in ^{1}H-^{1}H COSY. [e] HMBC correlations with the proton in the corresponding line in the HMBC experiments optimized for the 8.3 Hz of long-range J_{CH} value. [f] NOE correlations with the proton in the corresponding line in NOESY experiment.

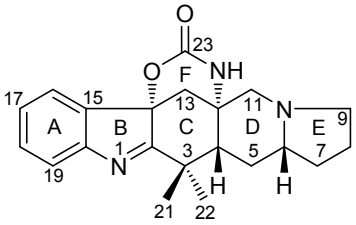

Penicimutamide C (**3**)

Table S6. 600 MHz ^{1}H and 150 MHz ^{13}C NMR data of **3** in acetone-d_6.[a]

No.	δ_C [b,c]	δ_H (J in Hz) [b]	COSY [d]	HMBC [e]	NOE [f]
2	187.6 s	—	—	—	—
3	40.0 s	—	—	—	—
4	53.4 d	1.60 dd (12.4, 2.1)	H_2-5	C-3,5,6,12,21,22	Hβ-5,11,13, H-6, H_3-21
5	28.5 t	Hα 1.54 q (11.3)	H-4, Ha-5, H-6	C-4,6,7,12	Hβ-5, Hα-7, H_3-22, N<u>H</u>
		Hβ 1.98–1.89 m	H-4, Hb-5, H-6	C-4,6,12	Hα-5, H-4,6, H_3-21,22
6	64.7 d	1.98–1.89 m	H_2-5, H_2-7	C-4,7,8	H-4, Hβ-5,7,9,11
7	31.0 t	Hα 1.58–1.48 m	H-6, Hβ-7, H_2-8	C-6,8,9	Hα-5, Hβ-7, Hα-8
		Hβ 1.98–1.89 m	H-6, Hα-7, Hβ-8	C-6,8,9	H-6, Hα-7, Hβ-8
8	22.3 t	Hα 1.87–1.78 m	Hα-7, Hβ-8, H_2-9	C-6,7,9	Hα-7,9, Hβ-8
		Hβ 1.74–1.68 m	H_2-7, Hα-8, H_2-9	C-6	Hβ-7,9, Hα-8
9	53.74 t	Hα 3.03 br t (8.6)	H_2-8, Hβ-9	C-6,7,8	Hα-8,11, Hβ-9
		Hβ 2.14 q (8.6)	H_2-8, Hα-9	C-8,11	H-6, Hβ-7,8,11, Hα-9
10	—	—	—	—	—
11	62.9 t	Hα 2.99 d (10.9)	—	C-4,6,9,12,13	Hα-9,13, Hβ-11, N<u>H</u>
		Hβ 2.20 d (10.9)		C-4,6,9,12,13	H-4,6, Hα-11, Hβ-13
12	53.79 s	—	—	—	—
13	38.7 t	Hα 2.48 d (14.2)	Hβ-13	C-2,4,5,11,12,14,15	Hα-11, Hβ-13, H-16, N<u>H</u>
		Hβ 1.75 d (14.2)	Hα-13	C-2,4,11,12,14,15	H-4, Hβ-11, Hα-13
14	87.1 s	—	—	—	—
15	137.8 s	—	—	—	—
16	123.8 d	7.52 ddd (7.5,1.2, 0.8)	H-17, 18	C-14,18,19,20	Hα-13, H-17
17	127.1 d	7.28 td (7.5, 0.8)	H-16, 18, 19	C-15,16,18,19,20	H-16,17
18	131.1 d	7.42 td (7.5, 1.2)	H-16, 17, 19	C-15,16,17,20	H-17,19
19	121.5 d	7.48 dt (7.5, 0.8)	H-17, 18	C-15,16,17	H-18
20	154.2 s	—	—	—	—
21	27.6 q	1.40 3H, s	H_3-22	C-2,3,4,22	H-4, Hβ-5, H_3-22
22	22.2 q	1.19 3H, s	H_3-21	C-2,3,4,21	H_2-5, H_3-21, N<u>H</u>
23	152.0 s	—	—	—	—
N<u>H</u>		6.26 s			Hα-5,11,13, H_3-22

[saa] Signals assignments were based on the results of DEPT, ^{1}H-^{1}H COSY, HMQC, and HMBC experiments. [b] Chemical shift values (δ_H and δ_C) were recorded using the solvent signals (CD_3COCD_3: δ_H 2.05/δ_C 29.84) as references, respectively. [c] Multiplicities of the carbon signals were determined by DEPT experiments and are indicated as s (singlet), d (doublet), t (triplet) and q (quartet), respectively. [d] The numbers in each line of this column indicate the protons that correlated with the proton in the corresponding line in ^{1}H-^{1}H COSY. [e] The numbers in each line of this column indicate the carbons that showed HMBC correlations with the proton in the corresponding line in the HMBC experiments optimized for the 8.3 Hz of long-range J_{CH} value. [f] Numbers in each line of this column indicate the protons that showed NOE correlations with the proton in the corresponding line in NOESY and 1D GOESY NOE experiment.

Figure S1. Measured CD for **1** in MeOH and calculated ECD for **1** and ***ent*-1**.

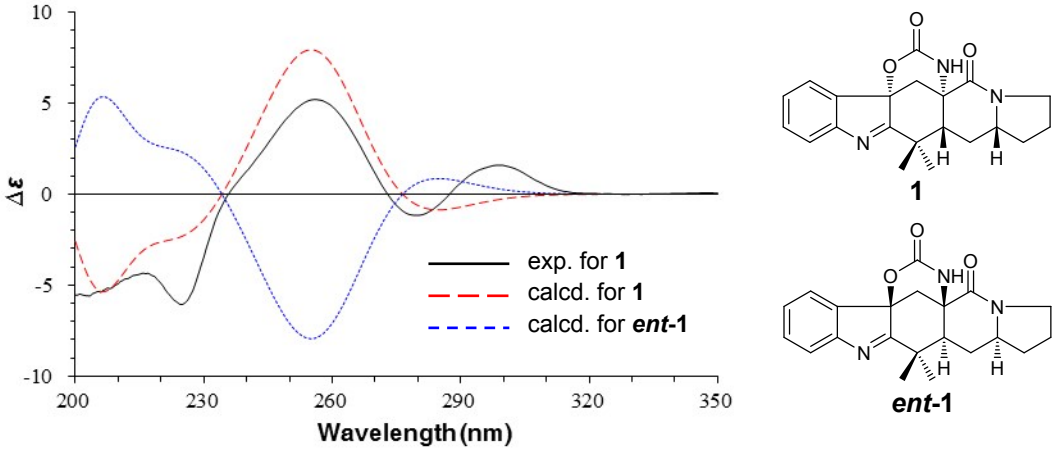

Figure S2. Measured CD for **2** in MeOH and calculated ECD for **2**/***ent*-2** and **4**/**4a**.

The CD spectrum of aspeverin (reported as **4a**) in MeOH in the literature (Ji, N.-Y.*et* al., *Org. Lett.* **2013**, *15*, 2327-2329) was almost identical to the CD spectrum of **2** in MeOH.

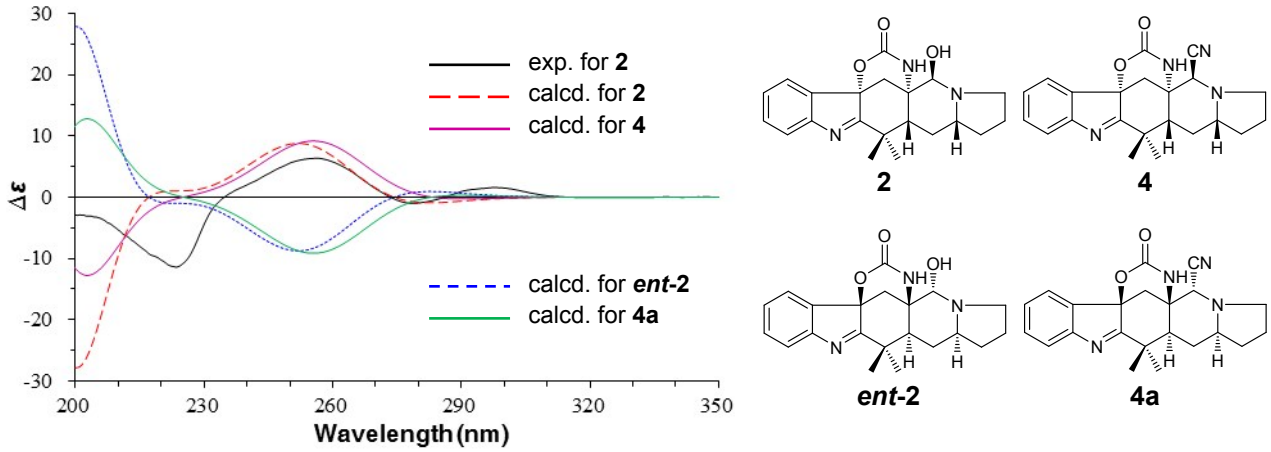

Figure S3. Measured CD for **3** in MeOH and calculated ECD for **3** and ***ent*-3**.

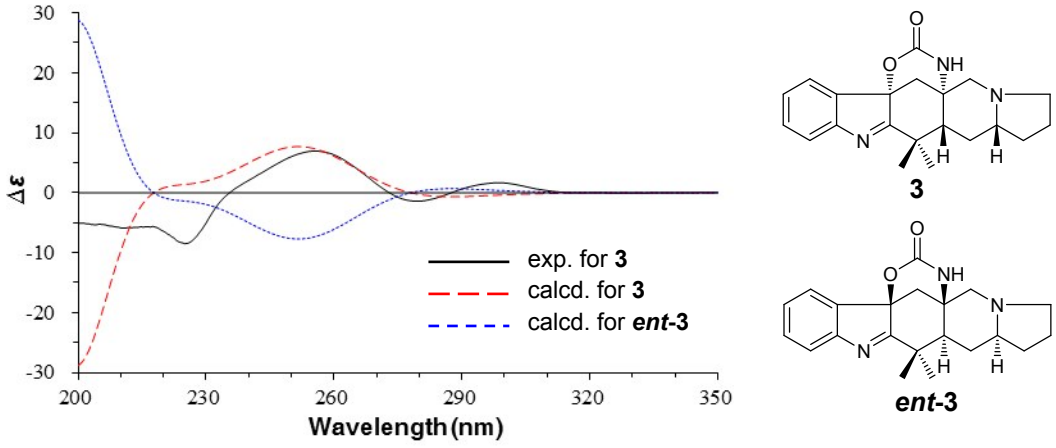

Figure S4. DFT-optimized structures of the low-energy conformers of **1** (A), ***ent*-1** (B), **2** (C), ***ent*-2** (D), **3** (E), ***ent*-3** (F), **4** (G) and **4a** (H) at the B3LYP/6-311+G(d) level in the gas phase (percentage in bracket: Boltzmann population calculated using the Gibbs free energy).

A: The low-energy conformers of **1**

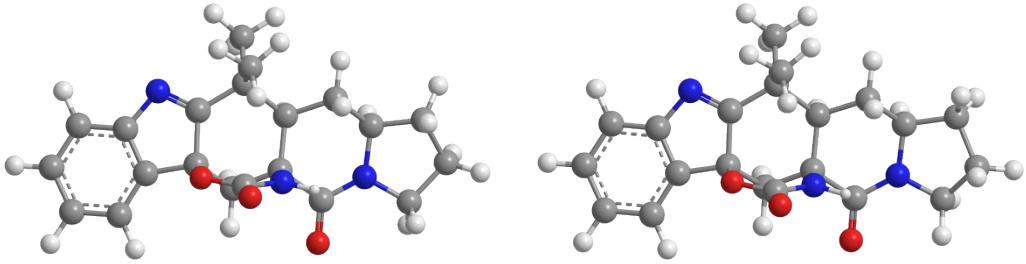

Conformer A (99%) Conformer B (1%)

B: The low-energy conformers of ***ent*-1**

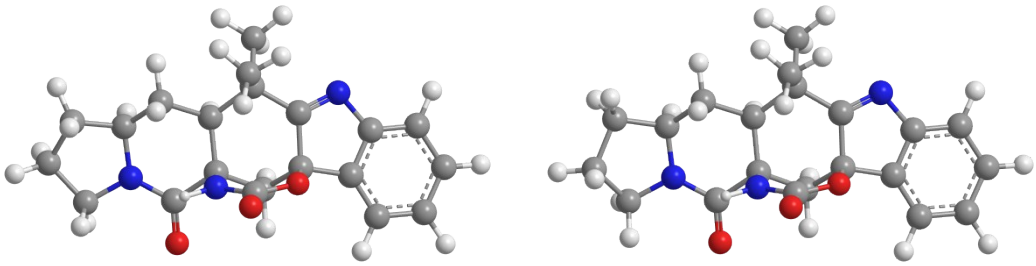

Conformer A (99%) Conformer B (1%)

C: The low-energy conformers of **2**

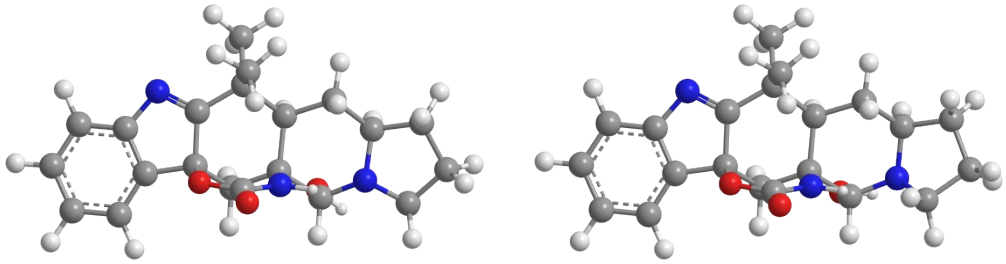

Conformer A (99%) Conformer B (1%)

D: The low-energy conformers of ***ent*-2**

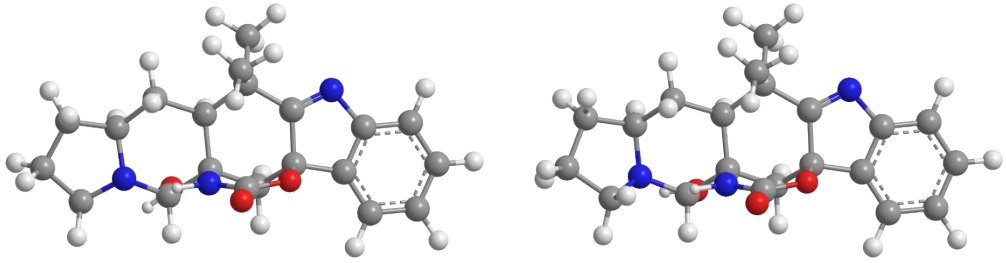

Conformer A (99%) Conformer B (1%)

Figure S4. *Continued*

E: The low-energy conformers of **3**

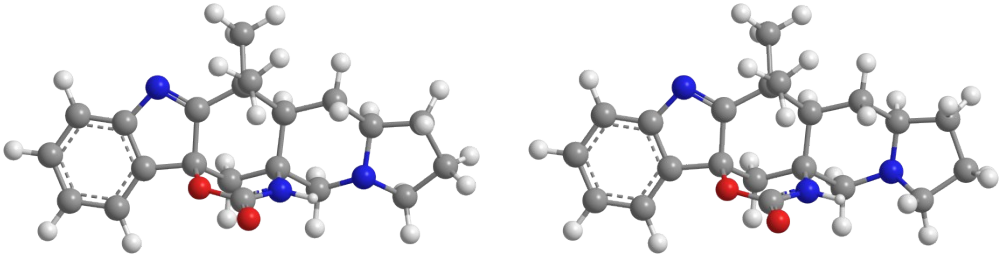

Conformer A (99%) Conformer B (1%)

F. The low-energy conformers of ***ent*-3**

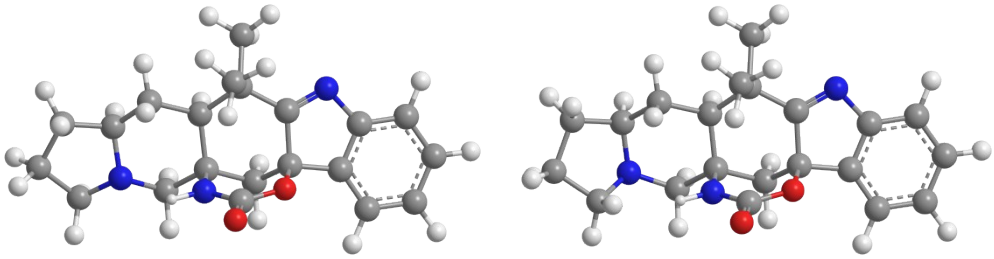

Conformer A (99%) Conformer B (1%)

G: The low-energy conformers of **4**

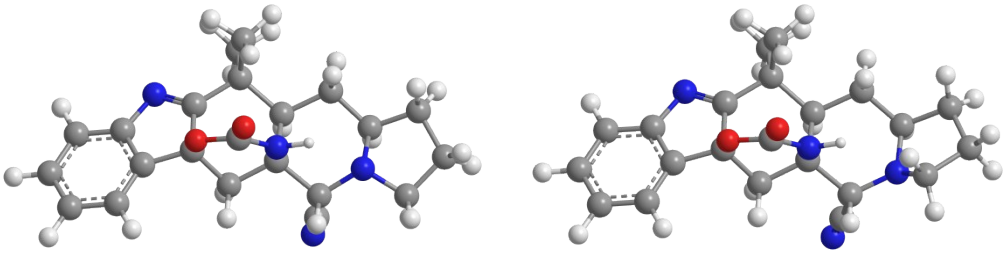

Conformer A (99%) Conformer B (1%)

H: The low-energy conformers of **4a**

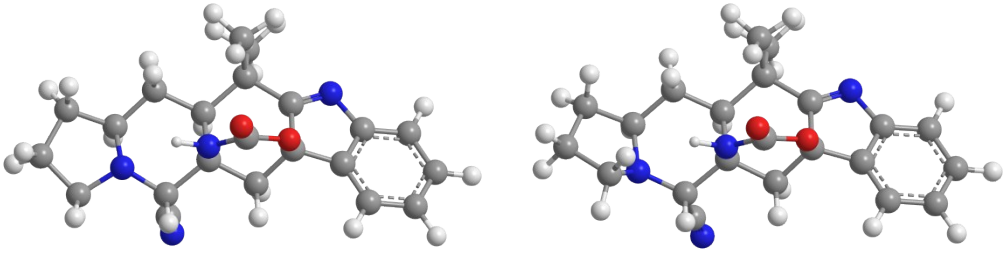

Conformer A (99%) Conformer B (1%)

Figure S5. HPLC-PDAD-UV analysis of the MeOH extracts of the mutant AD-2-1 and parent G59 strains to detect **1**–**3**.

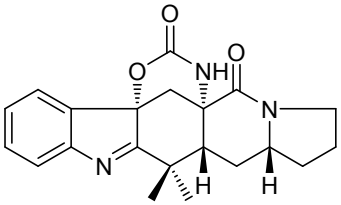

Penicimutamide A (**1**)

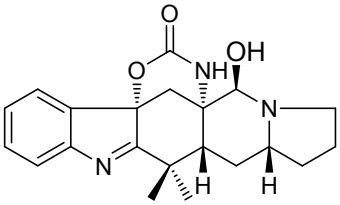

Penicimutamide B (**2**)

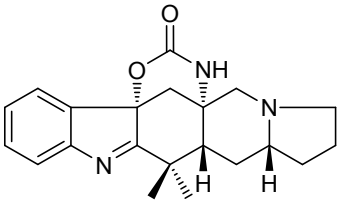

Penicimutamide C (**3**)

A: HPLC profiles of **1**–**3** and the MeOH extracts of the mutant AD-2-1 and parent G59 strains

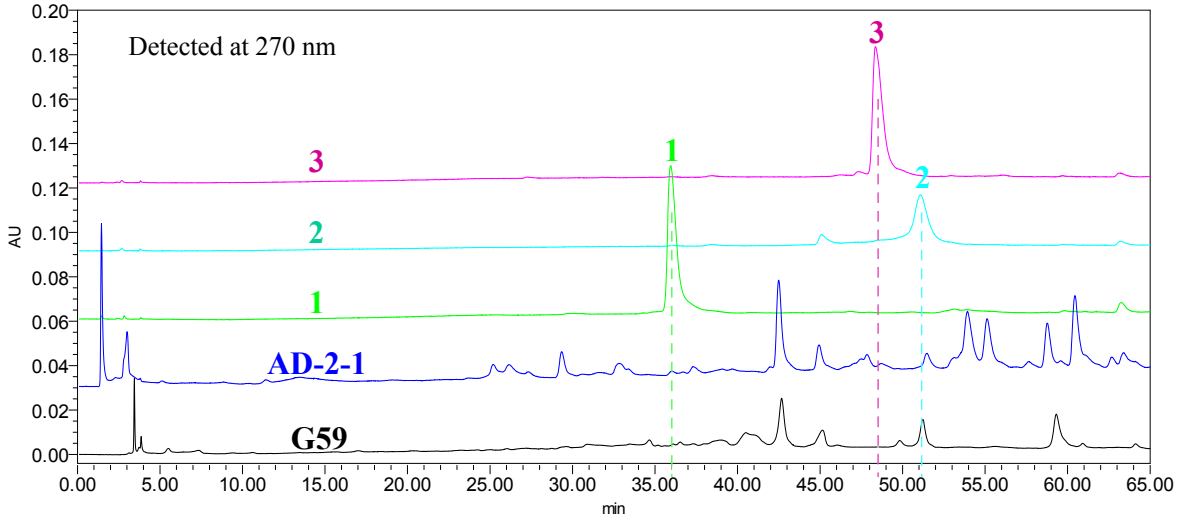

B: UV spectra of **1**–**3** and the AD-2-1 and G59 extracts at the given retention times (t_R)

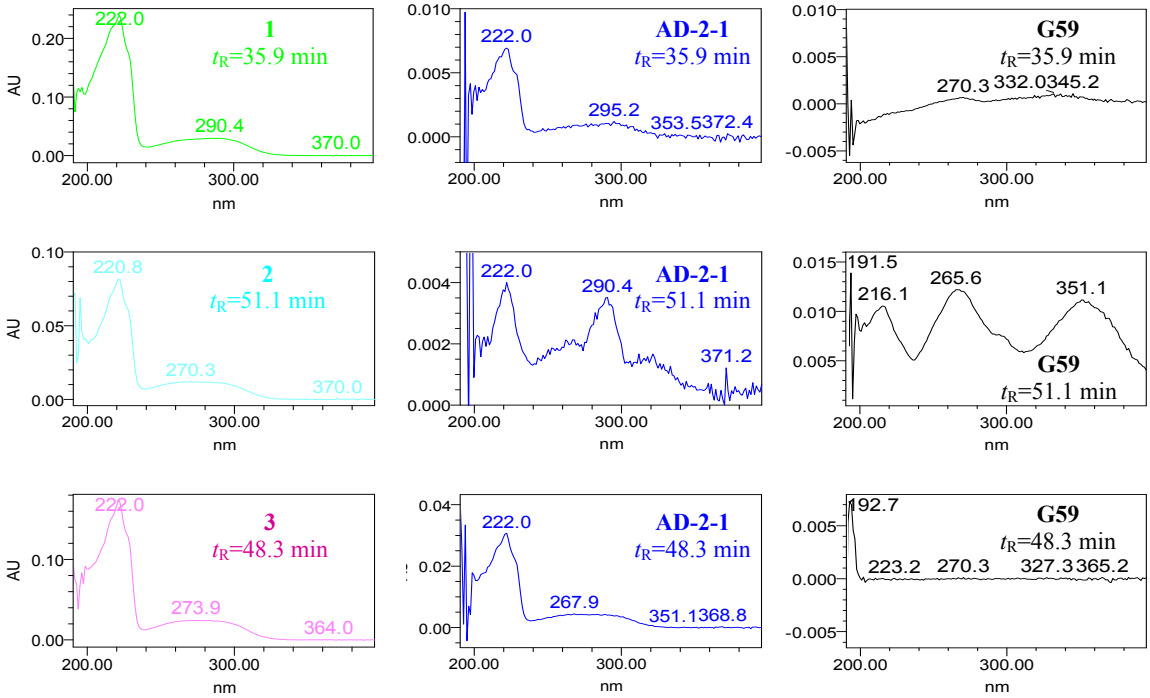

Figure S6. HPLC-ESI-MS analysis of the MeOH extracts of the mutant **AD-2-1** and parent **G59** strains to detect **1**–**3**.

A: HPLC-Positive ion ESI-MS analysis (ESIMS *m/z*: 388 $[M + Na]^+$ for **1**)

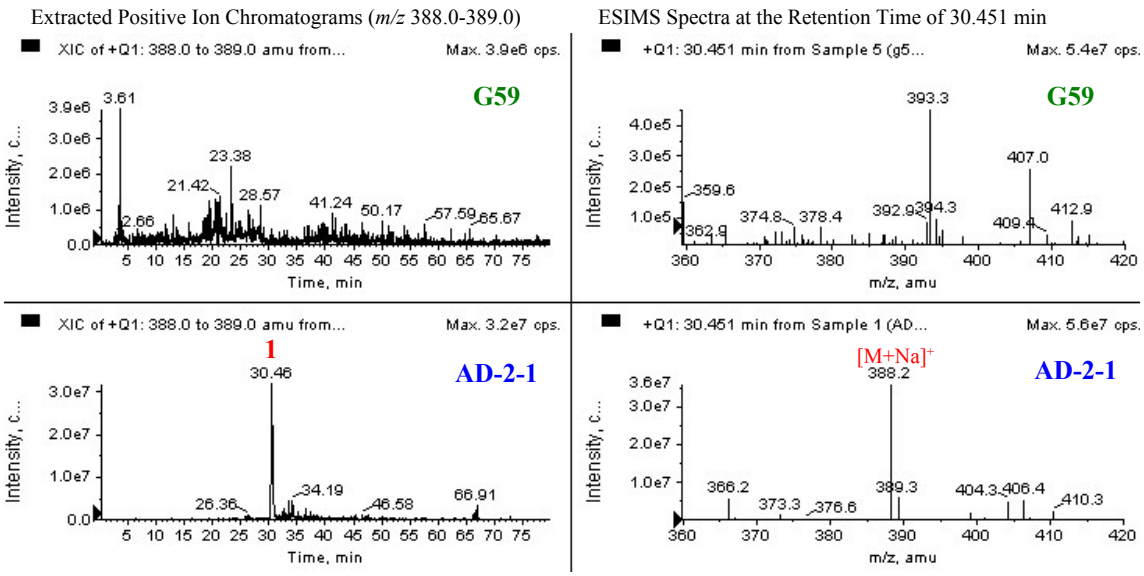

B: HPLC-Positive ion ESI-MS analysis (ESIMS *m/z*: 368 $[M + H]^+$ for **2**)

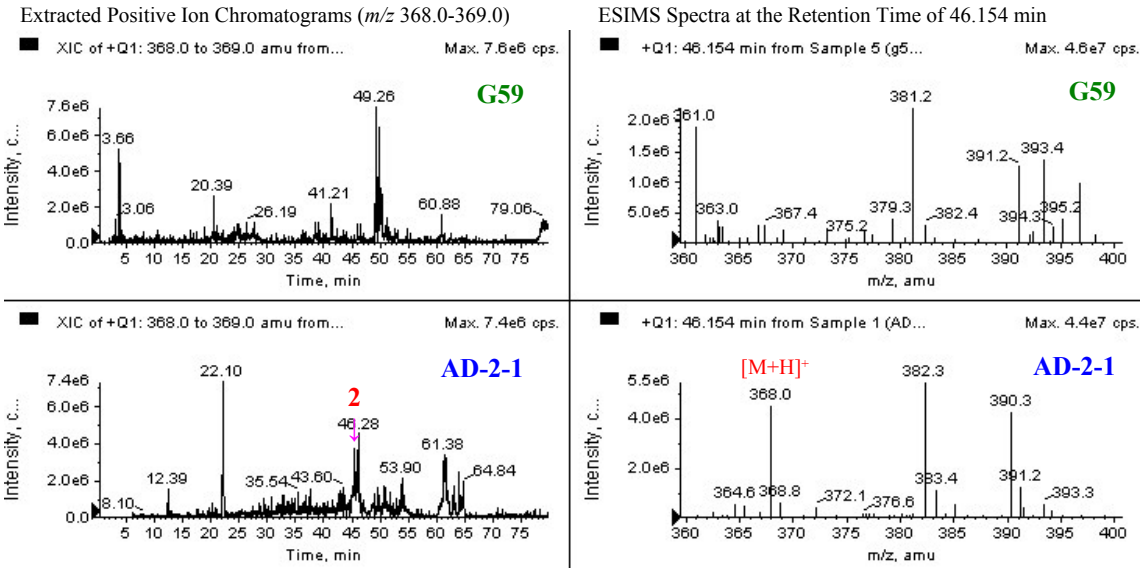

C: HPLC-Positive ion ESI-MS analysis (ESIMS *m/z*: 352 $[M + H]^+$ for **3**)

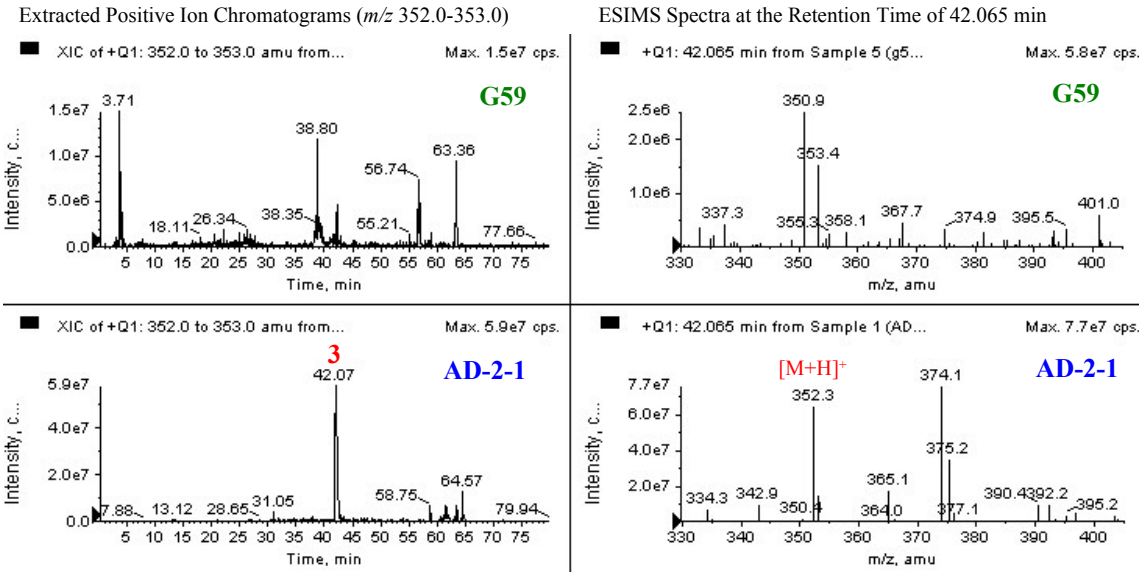

Figure S7. Positive (**A**) and negative (**B**) ion ESI-MS spectra of **1**.

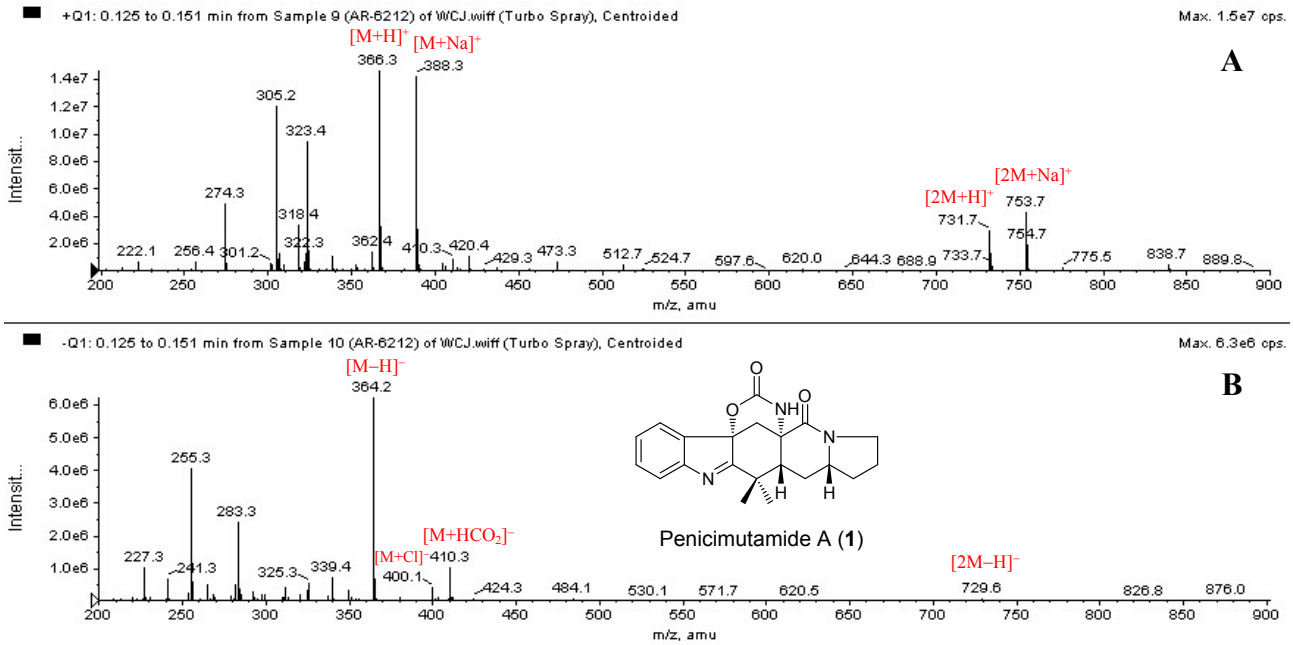

Figure S8. Positive ion HR-ESI-MS spectrum of **1**.

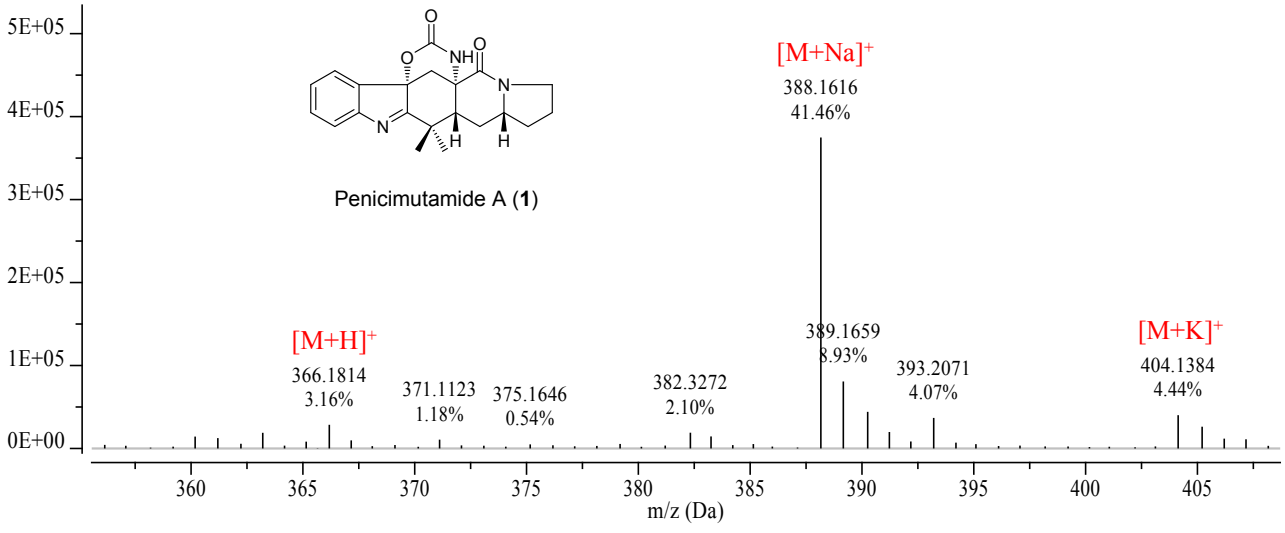

Figure S9. UV spectrum of **1** in MeOH.

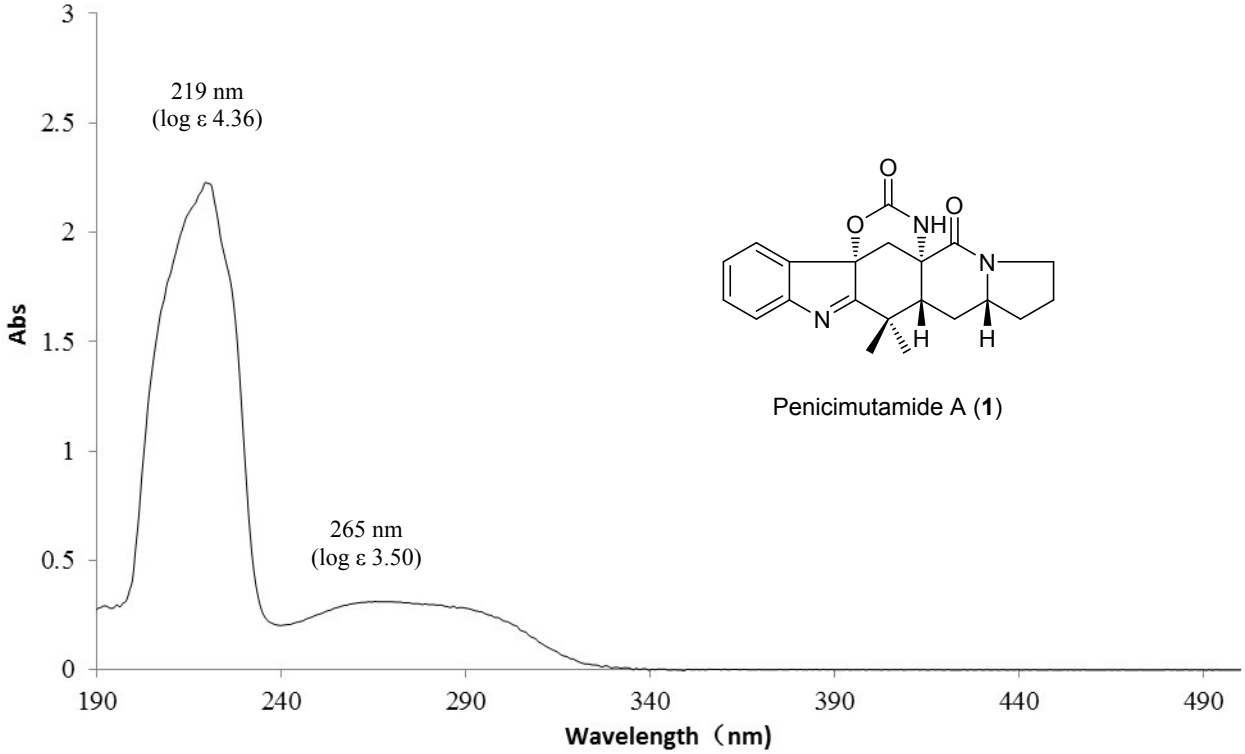

Figure S10. IR spectrum of **1** (measured on a diamond ATR crystal).

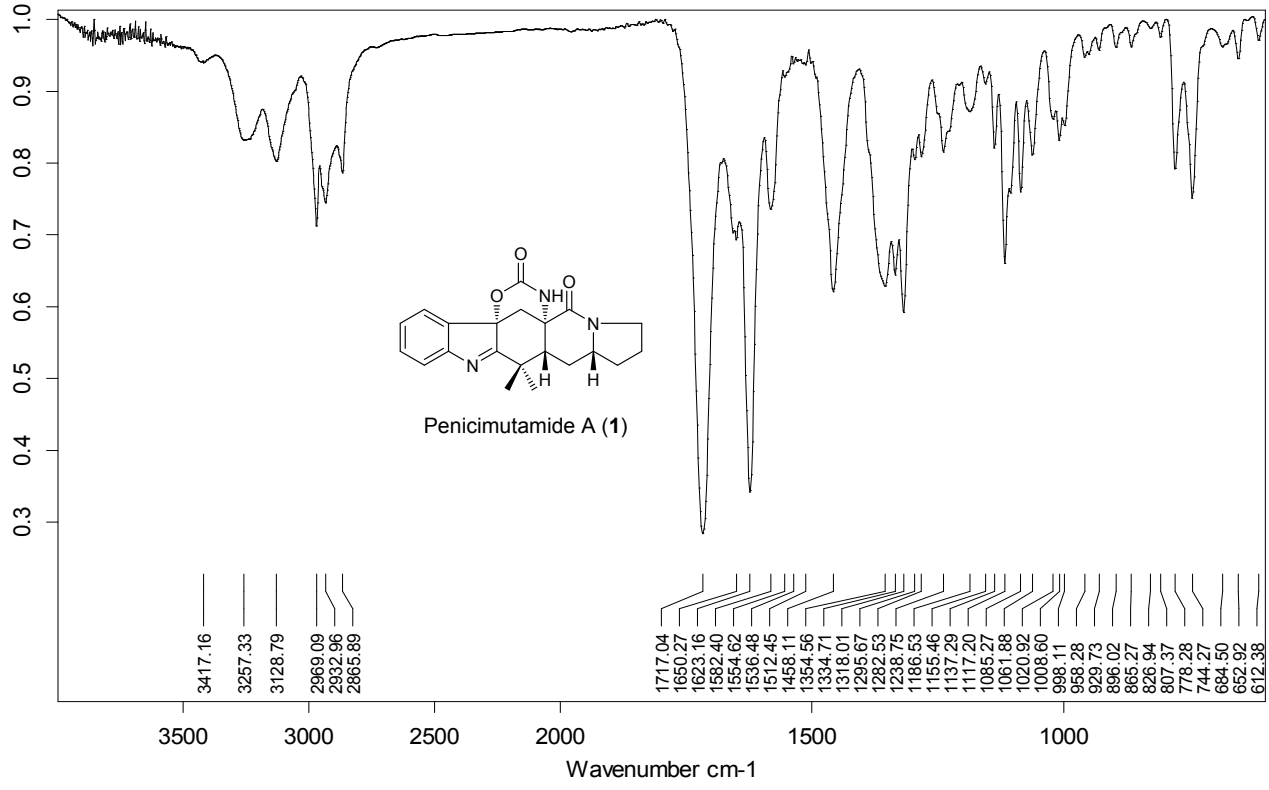

Figure S11. 600 MHz ^{1}H NMR spectrum of **1** in CD_3OD.

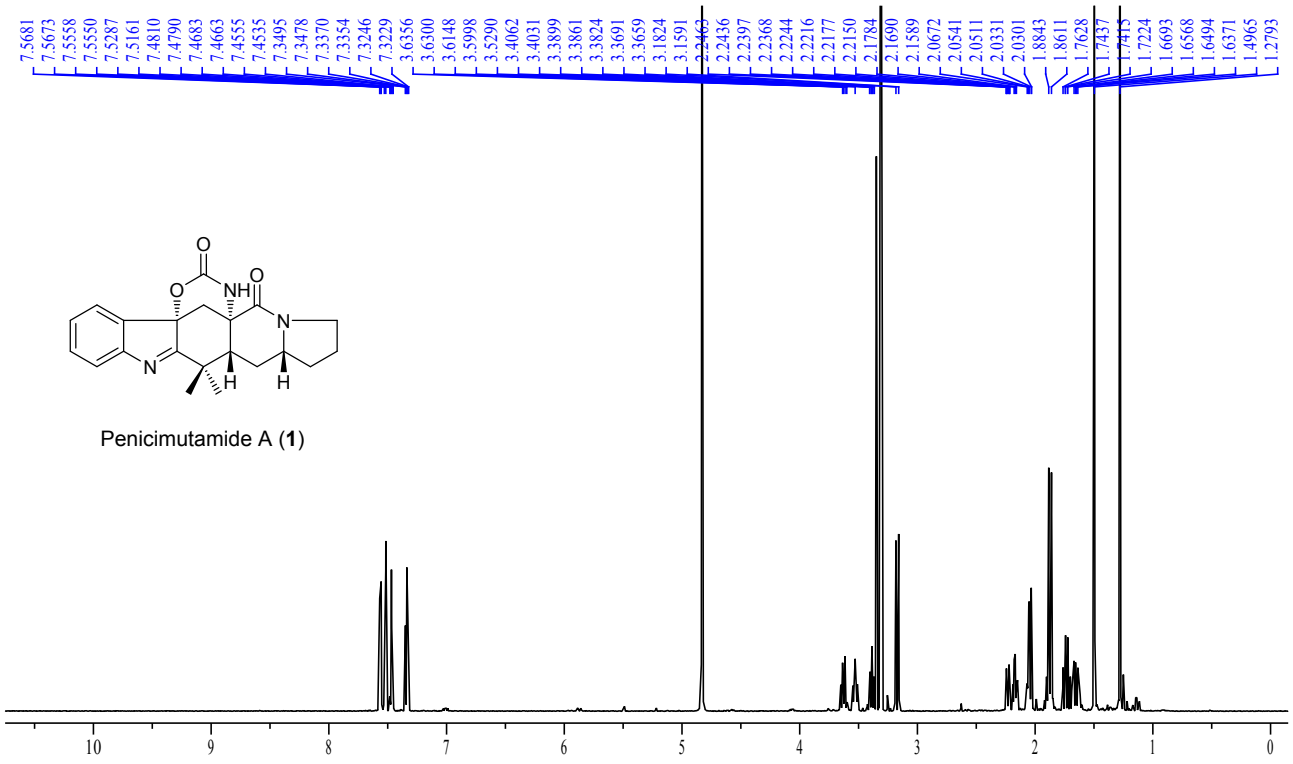

Figure S12. Enlarged 600 MHz ^{1}H NMR spectrum of **1** in CD_3OD.

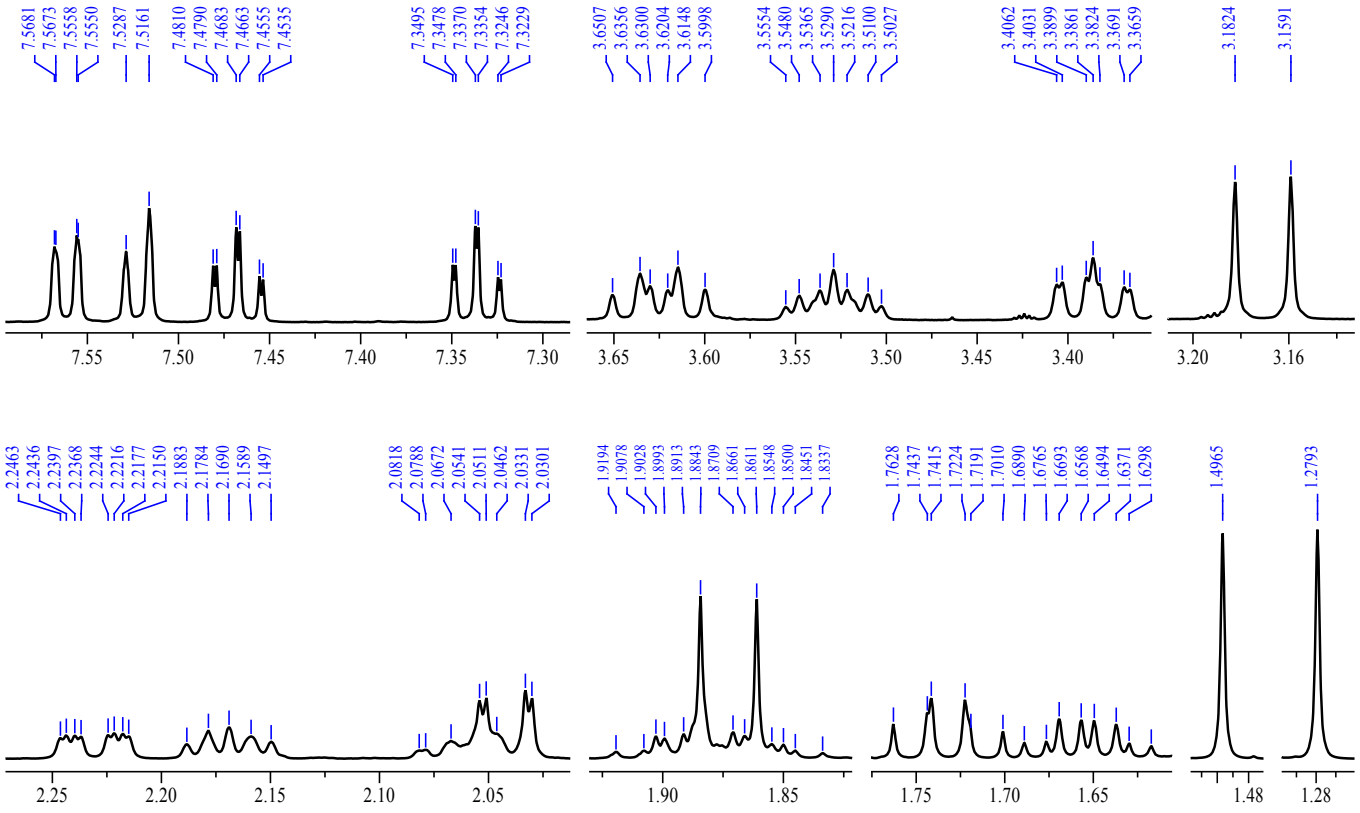

Figure S13. 150 MHz ^{13}C NMR spectrum of **1** in CD_3OD.

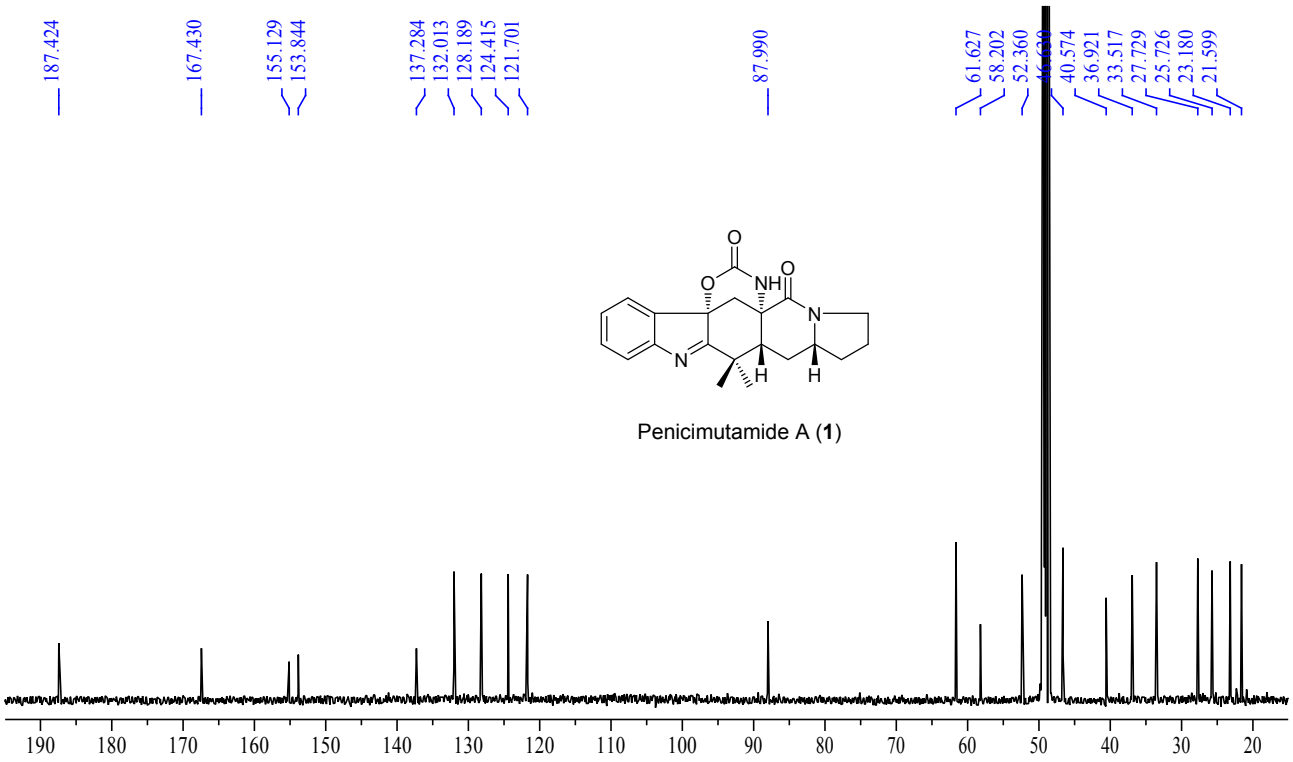

Figure S14. 150 MHz DEPT spectra of **1** in CD_3OD.

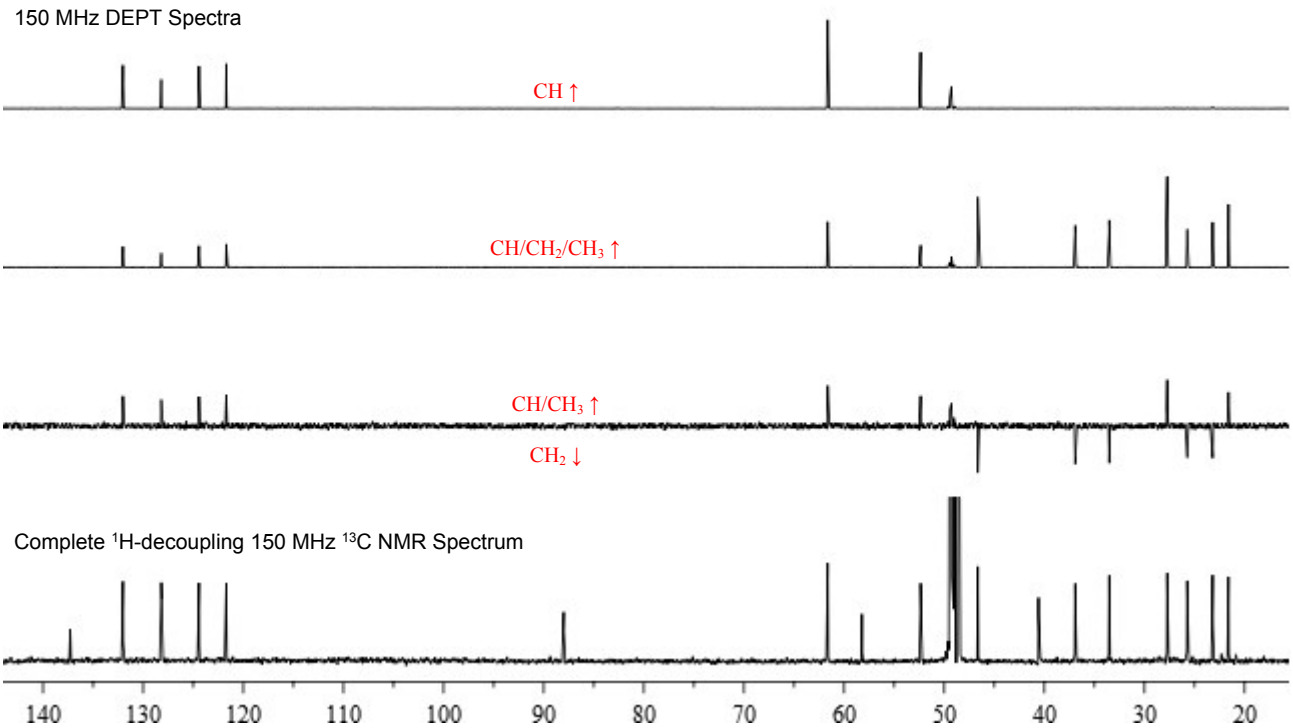

Figure S15. 600 MHz ^{1}H-^{1}H COSY spectrum of **1** in CD_3OD.

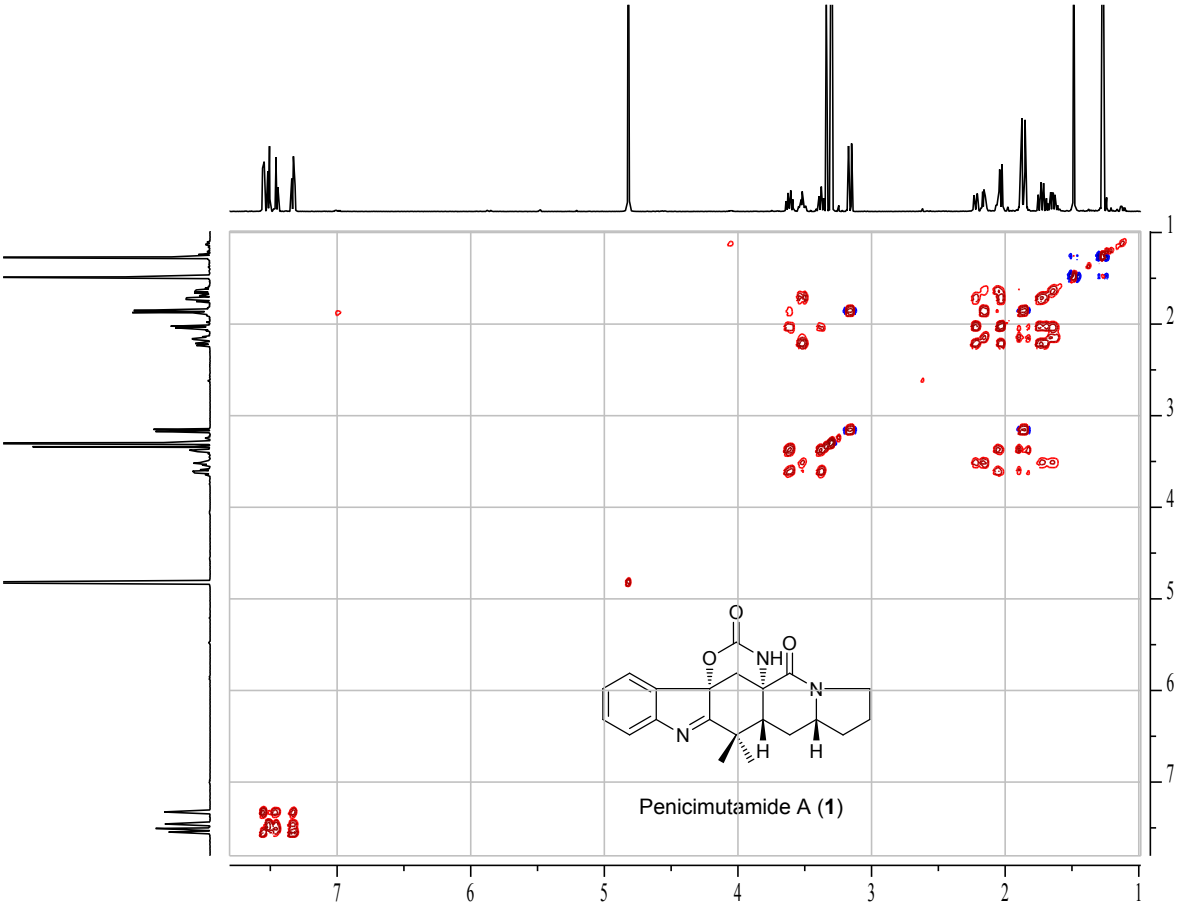

Figure S16. 600 MHz ^{1}H/150 MHz ^{13}C HMQC spectrum of **1** in CD_3OD.

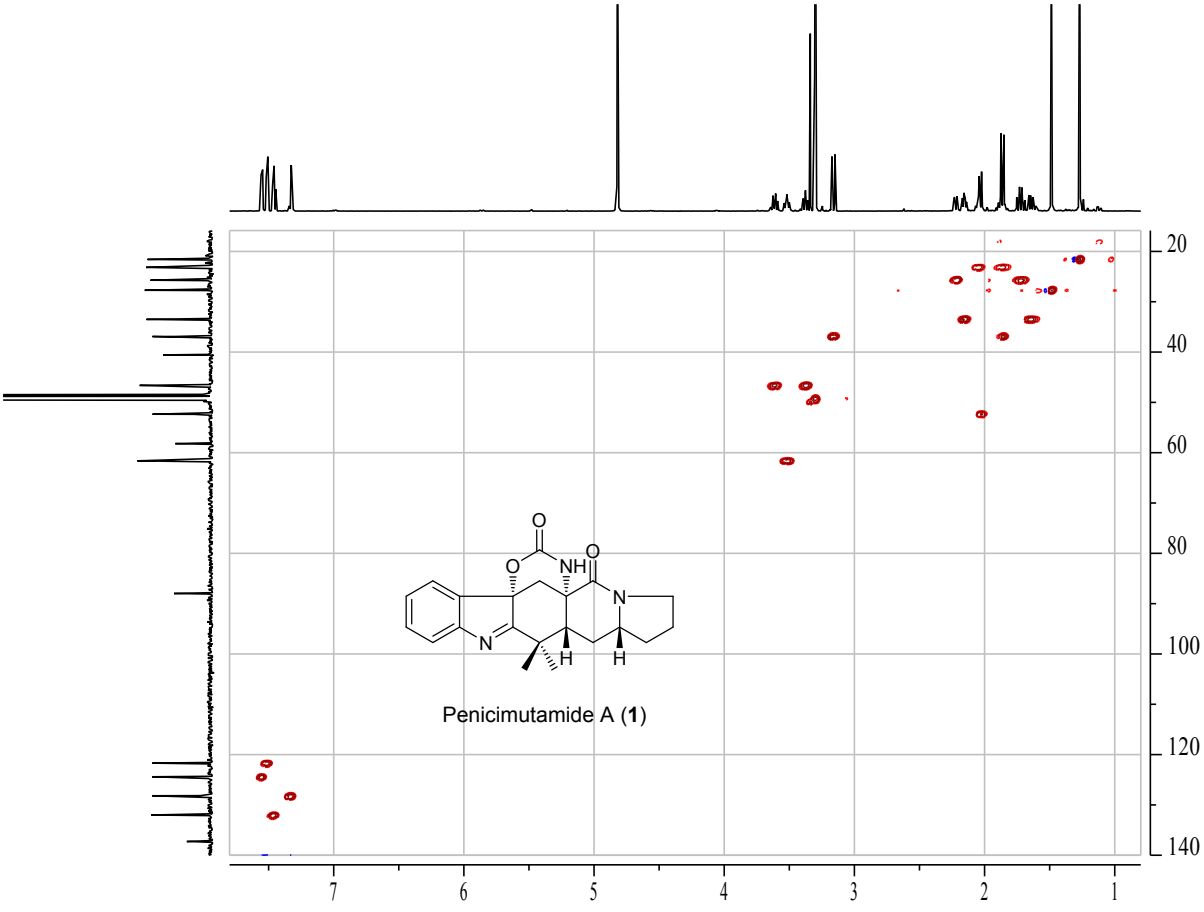

Figure S17. 600 MHz ^{1}H/150 MHz ^{13}C HMBC spectrum of **1** in CD_3OD.

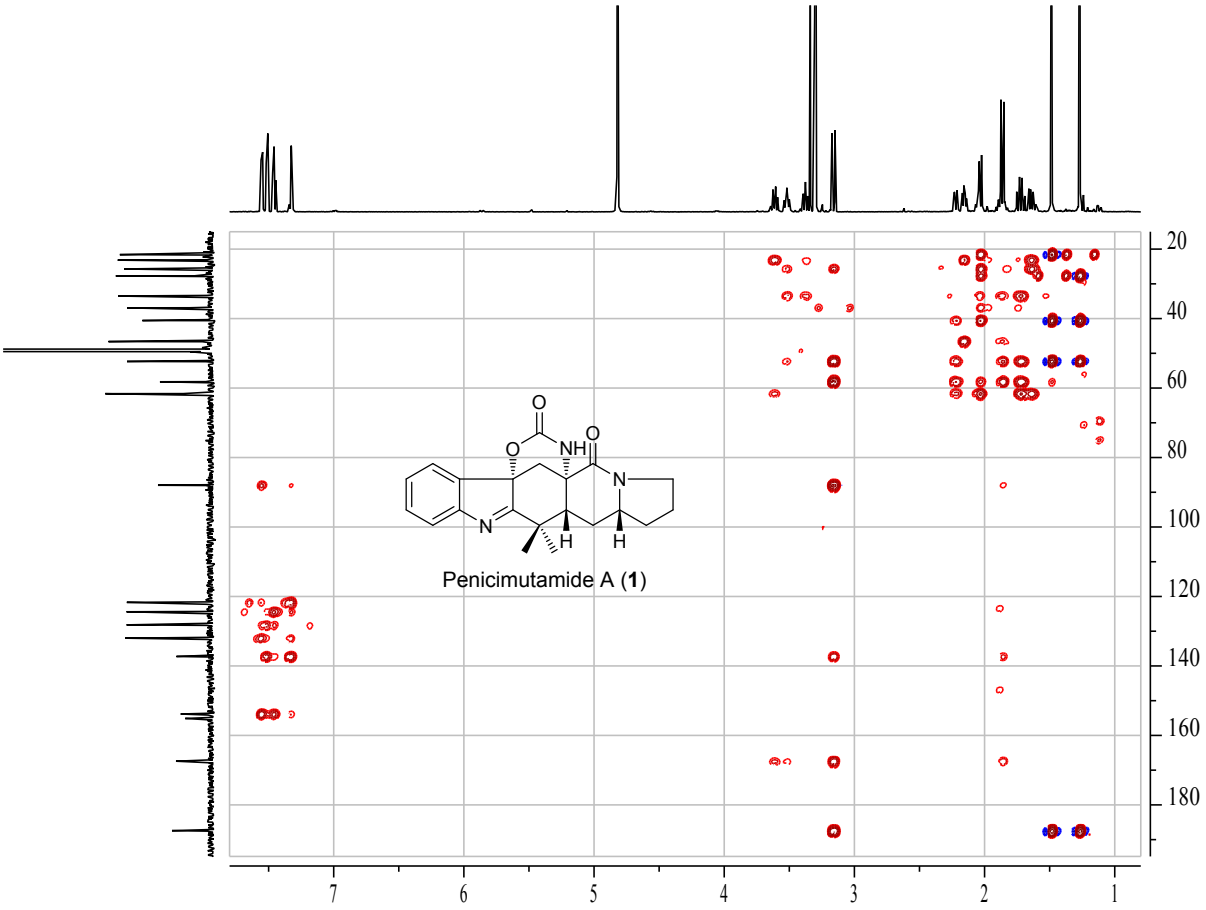

Figure S18. 600 MHz NOESY spectrum of **1** in CD_3OD.

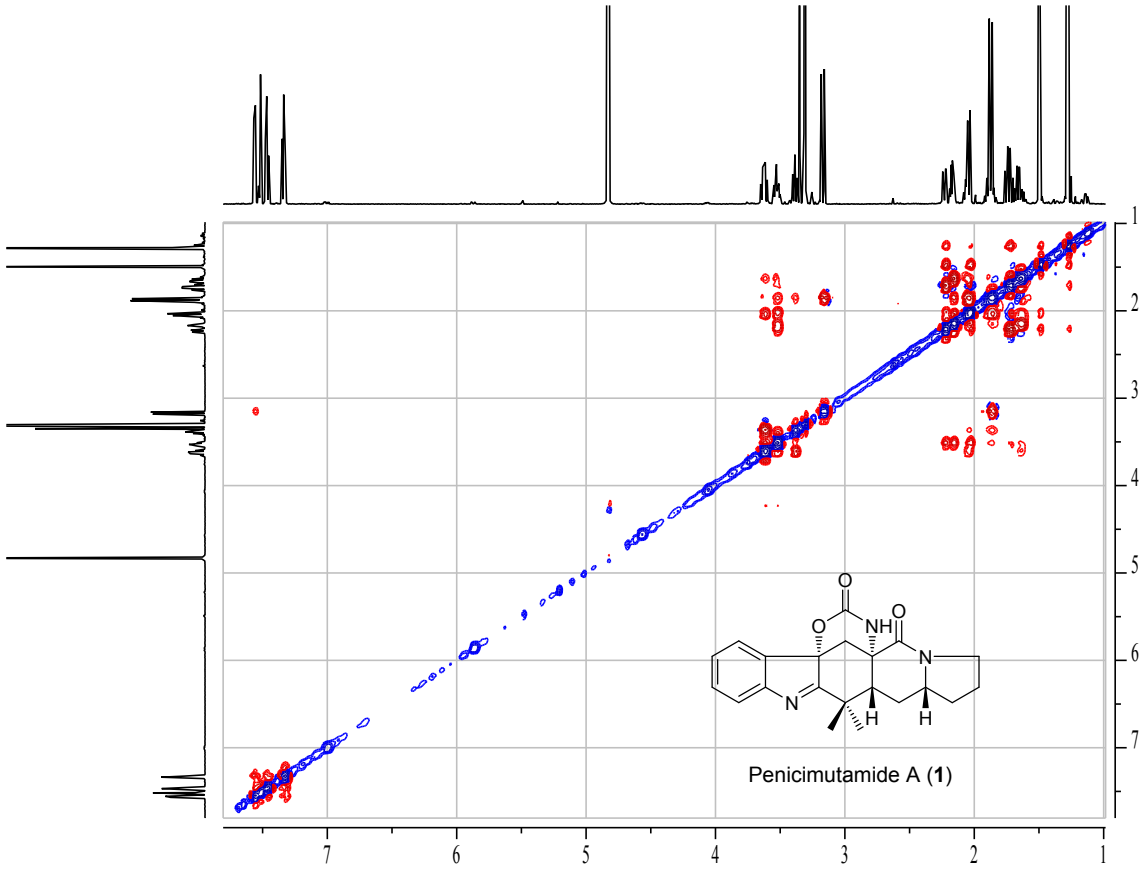

Figure S19. Positive (A) and negative (B) ion ESI-MS spectra of **2**.

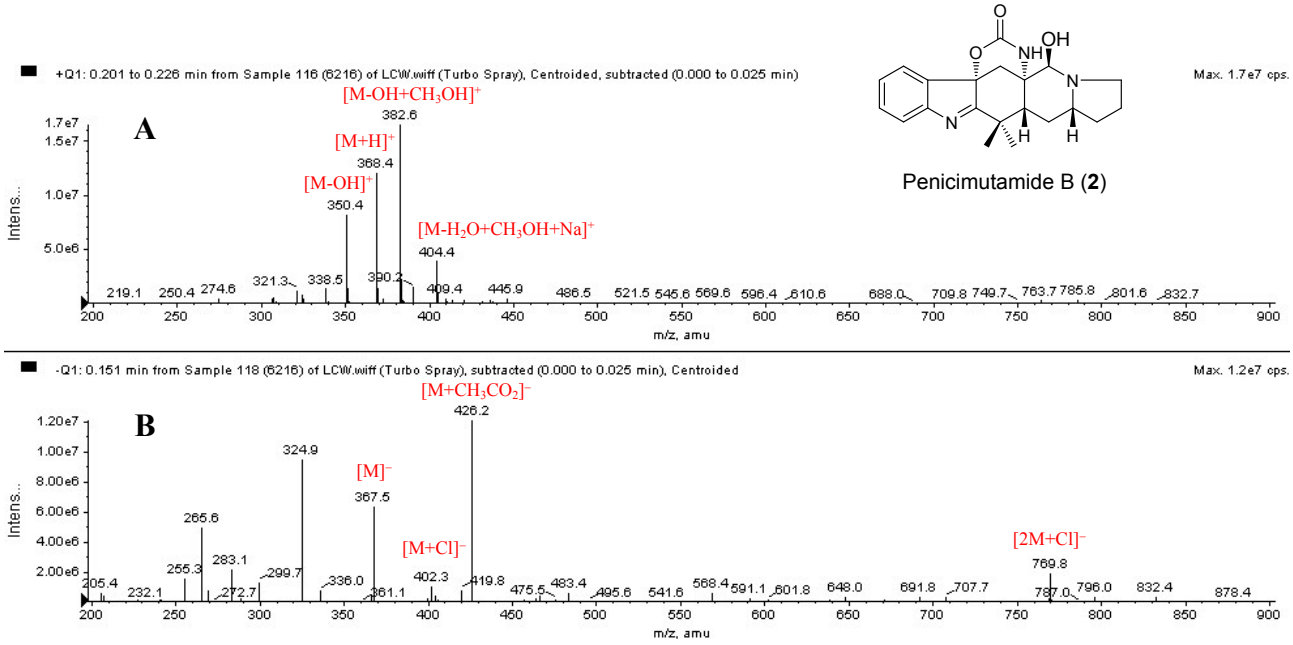

Figure S20. Positive ion HR-ESI-MS spectrum of **2**.

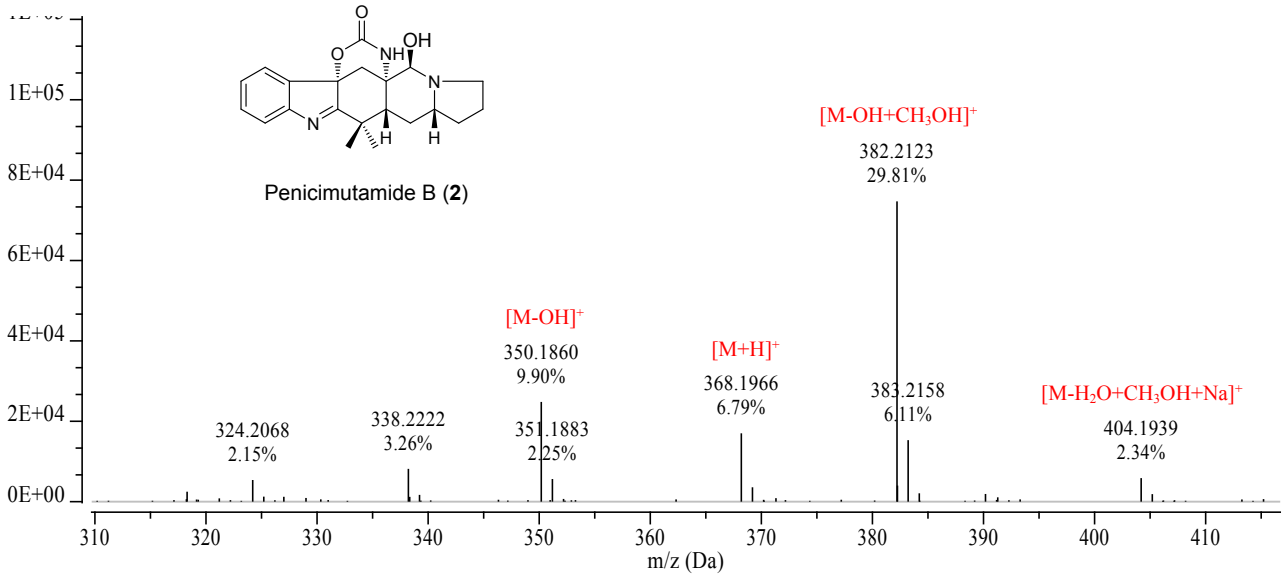

Figure S21. UV spectrum of **2** in MeOH.

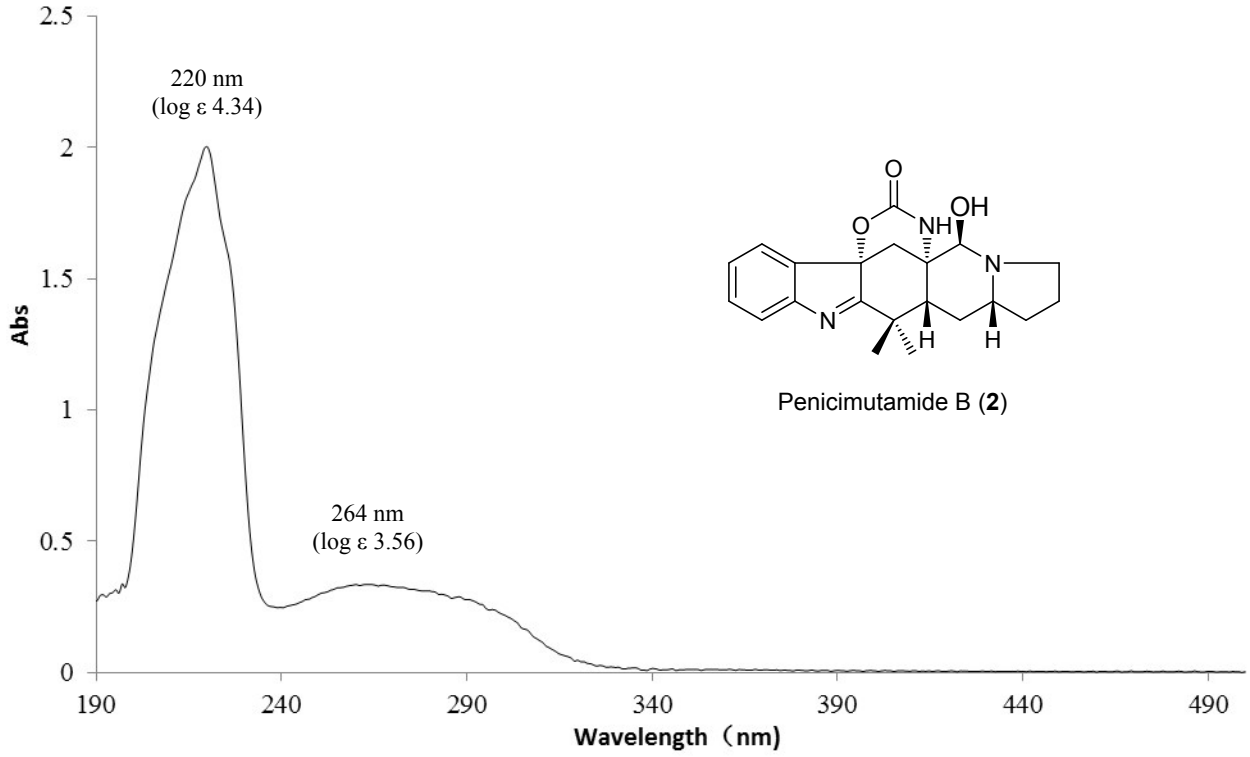

Figure S22. IR spectrum of **2** (measured on a diamond ATR crystal).

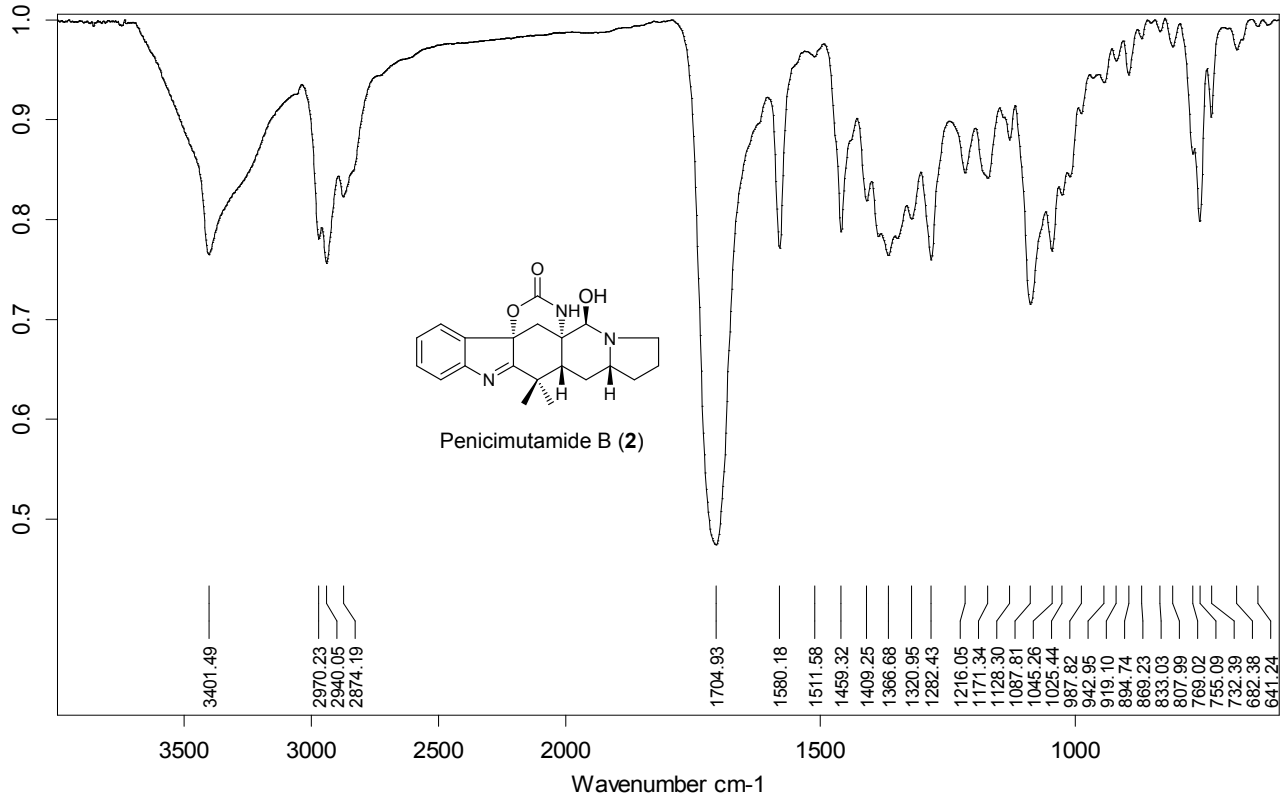

Figure S23. 600 MHz ^{1}H NMR spectrum of **2** in CD_3OD.

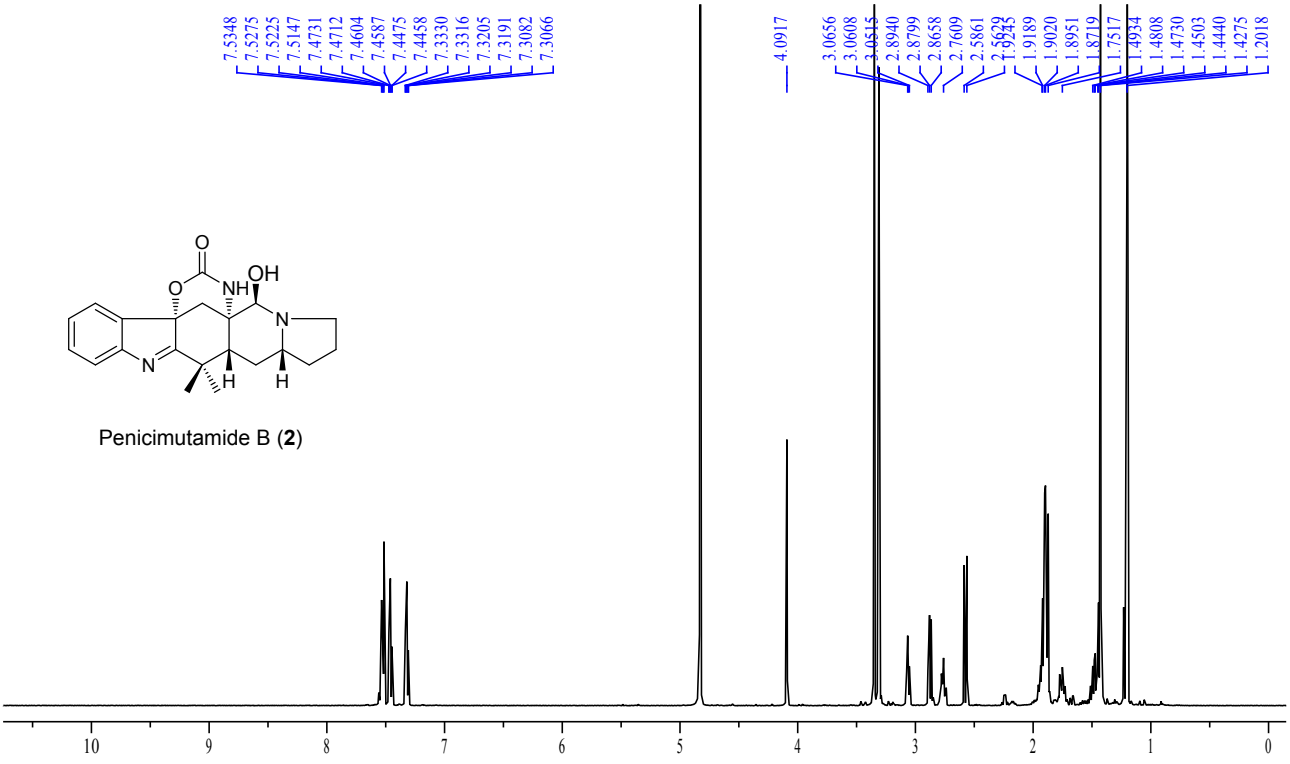

Figure S24. Enlarged 600 MHz ^{1}H NMR spectrum of **2** in CD_3OD.

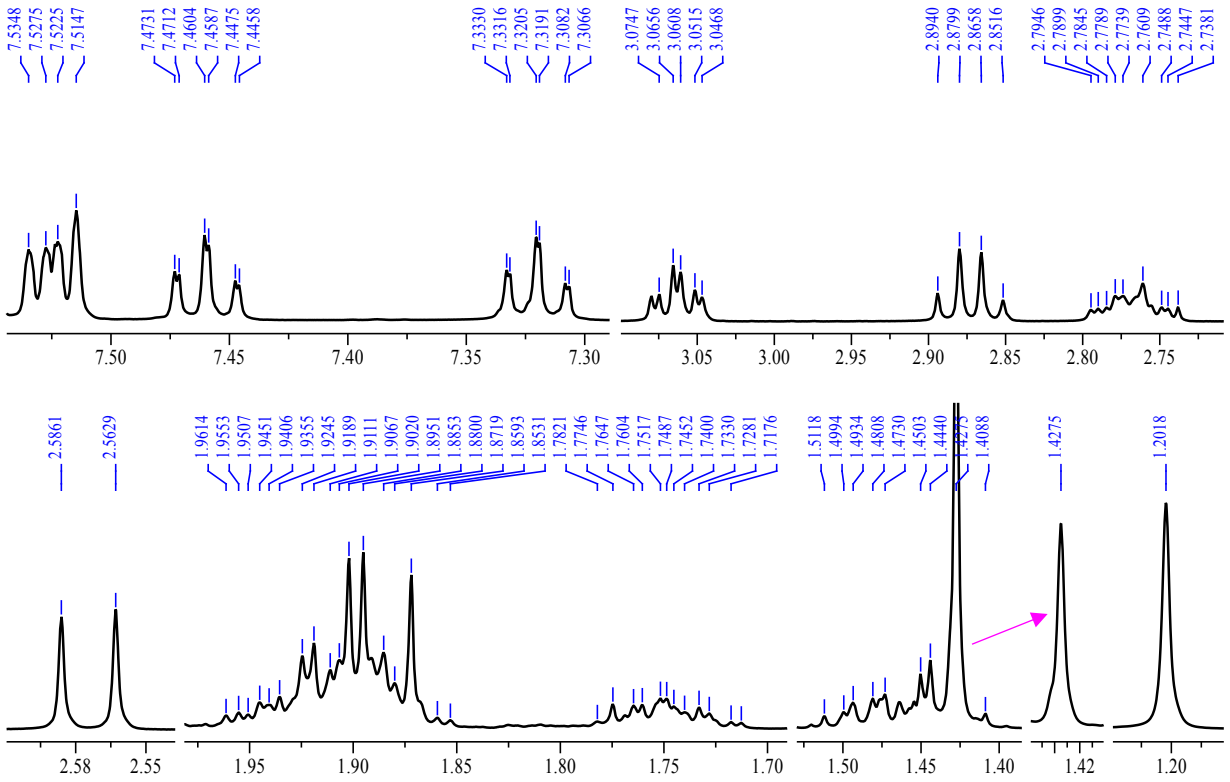

Figure S25. 150 MHz ^{13}C NMR spectrum of **2** in CD_3OD.

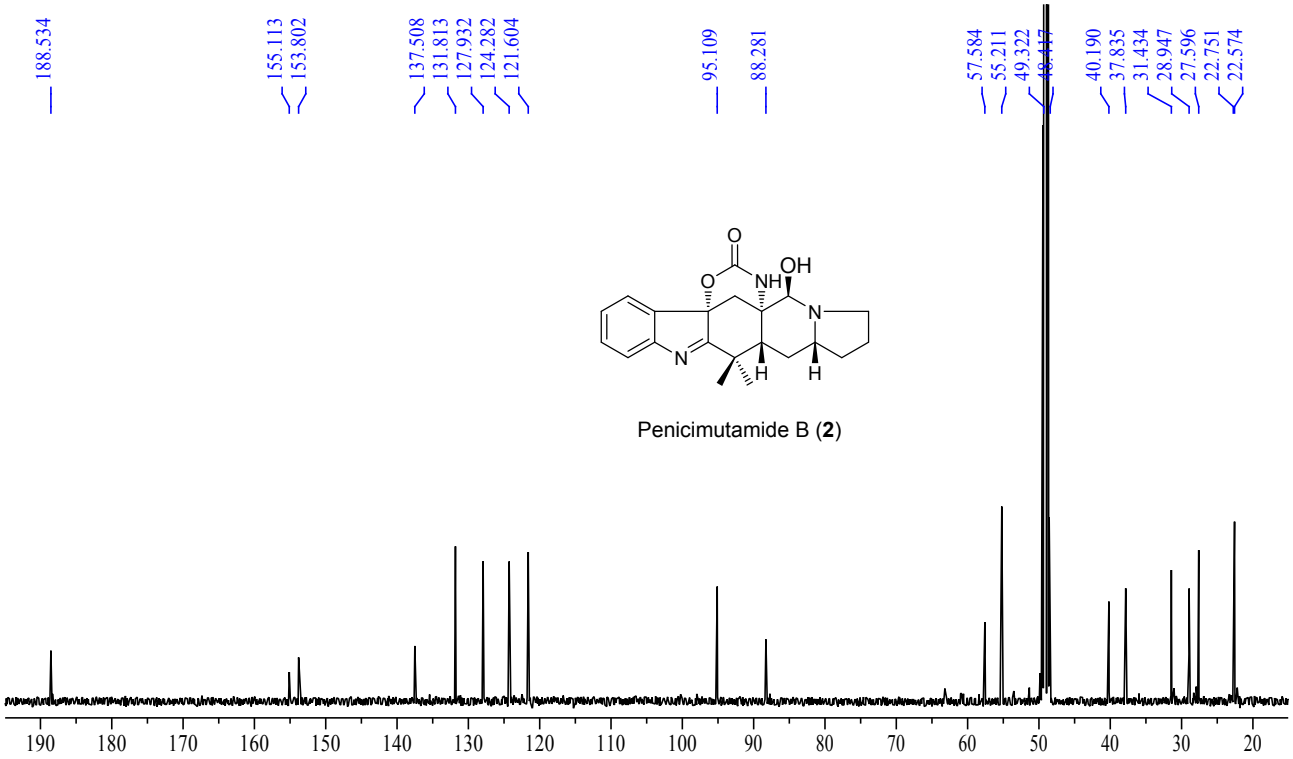

Figure S26. 150 MHz DEPT spectra of **2** in CD_3OD.

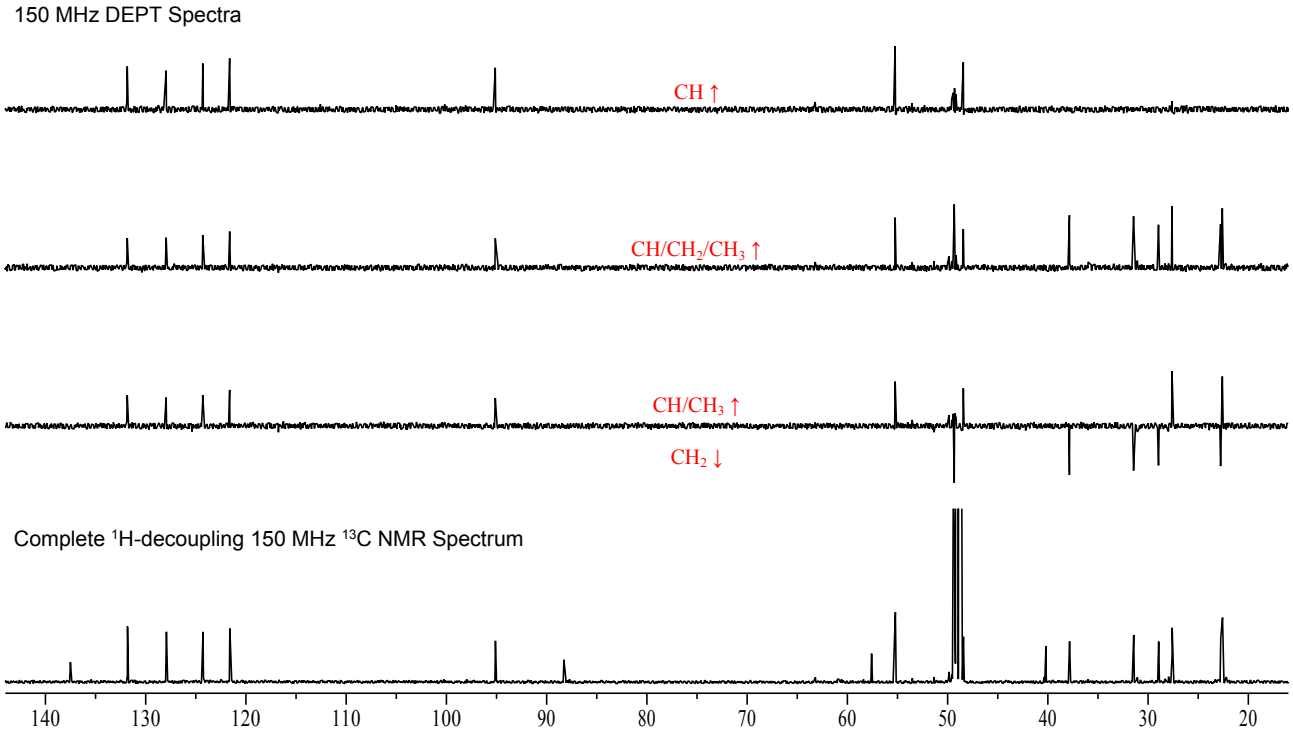

Figure S27. 600 MHz ^{1}H-^{1}H COSY spectrum of **2** in CD_3OD.

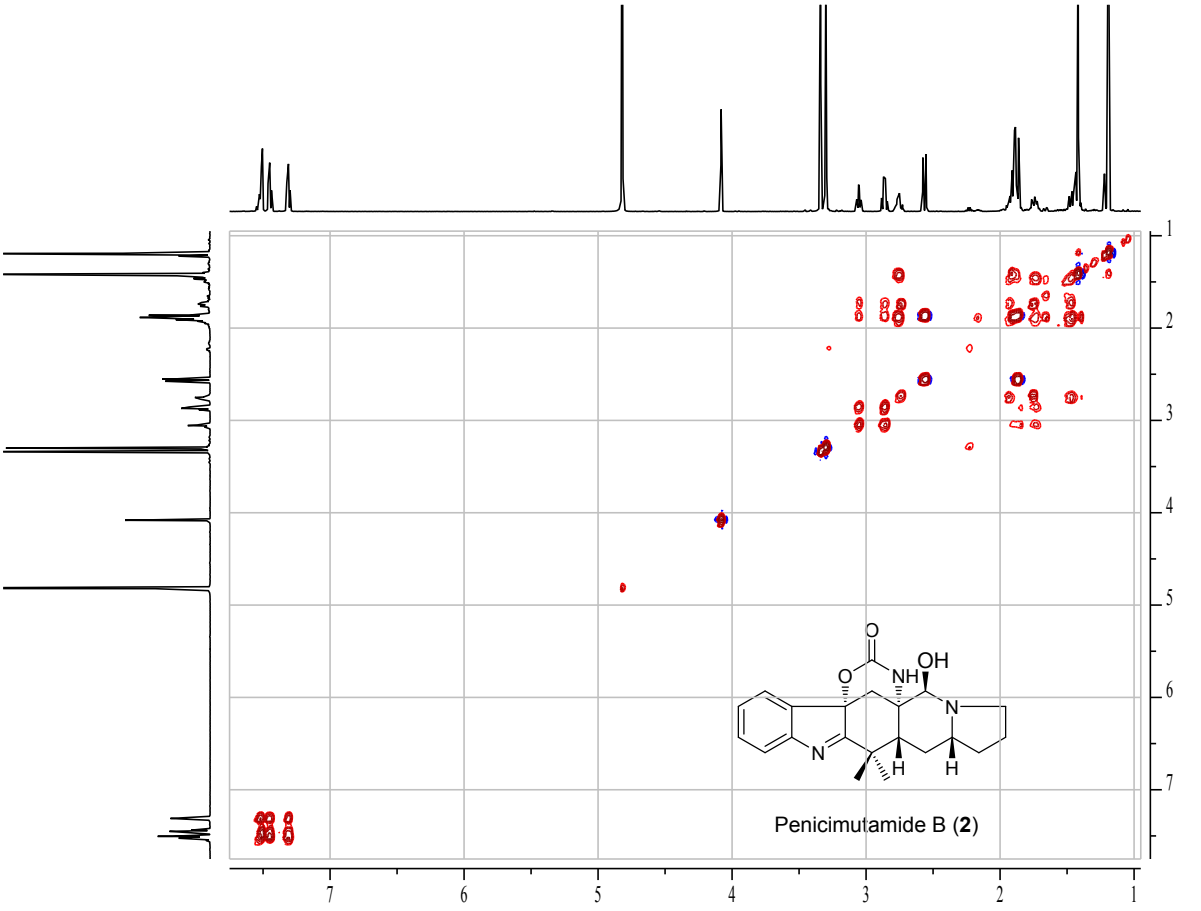

Figure S28. 600 MHz ^{1}H/150 MHz ^{13}C HMQC spectrum of **2** in CD_3OD.

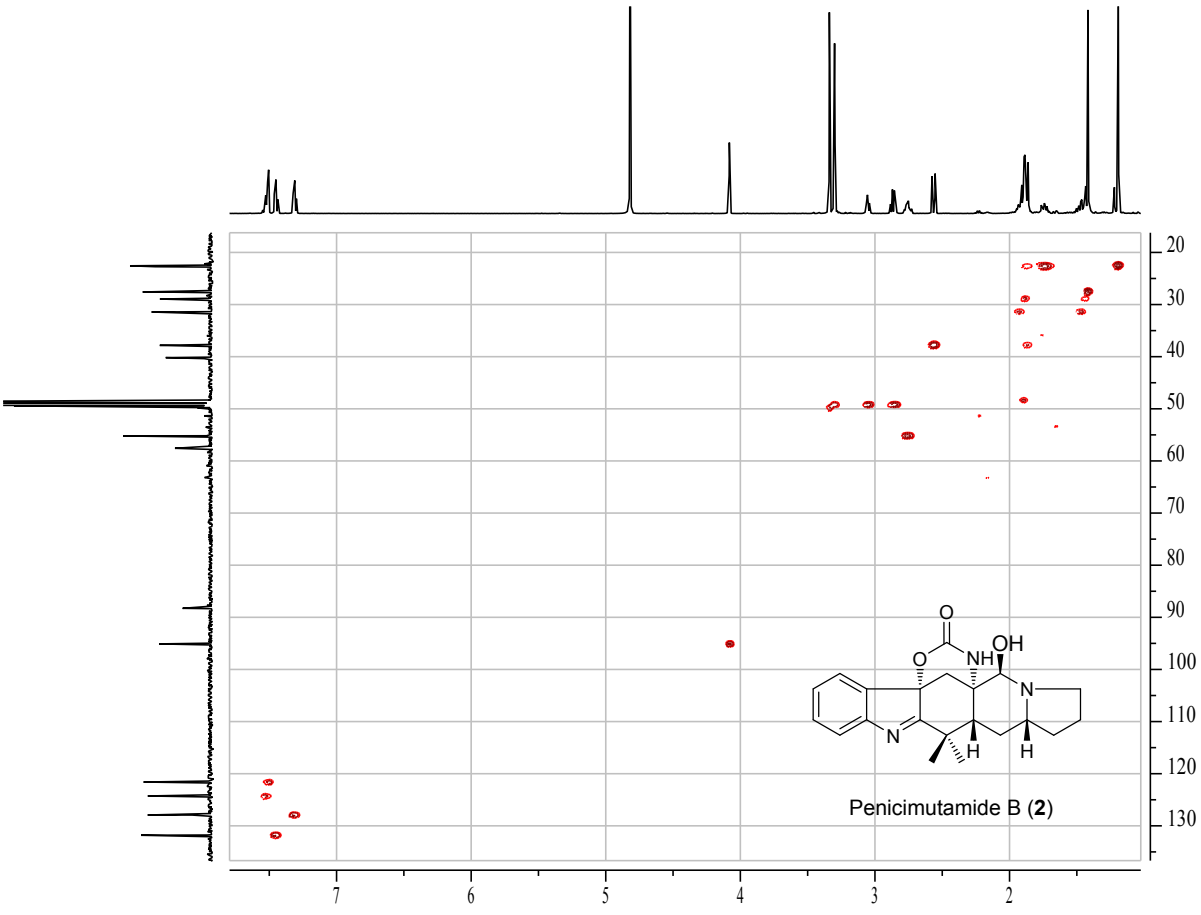

Figure S29. 600 MHz ^{1}H/150 MHz ^{13}C HMBC spectrum of **2** in CD_3OD.

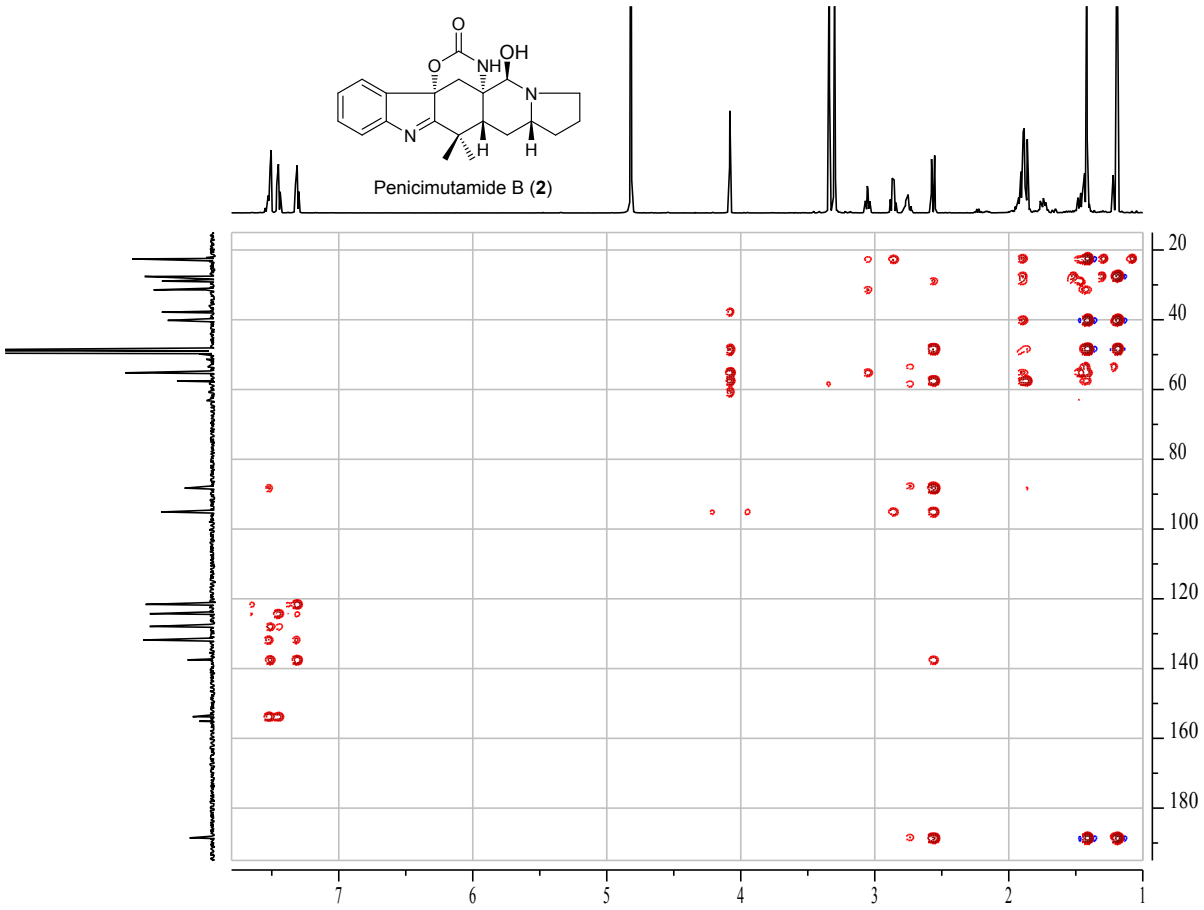

Figure S30. 600 MHz NOESY spectrum of **2** in CD_3OD.

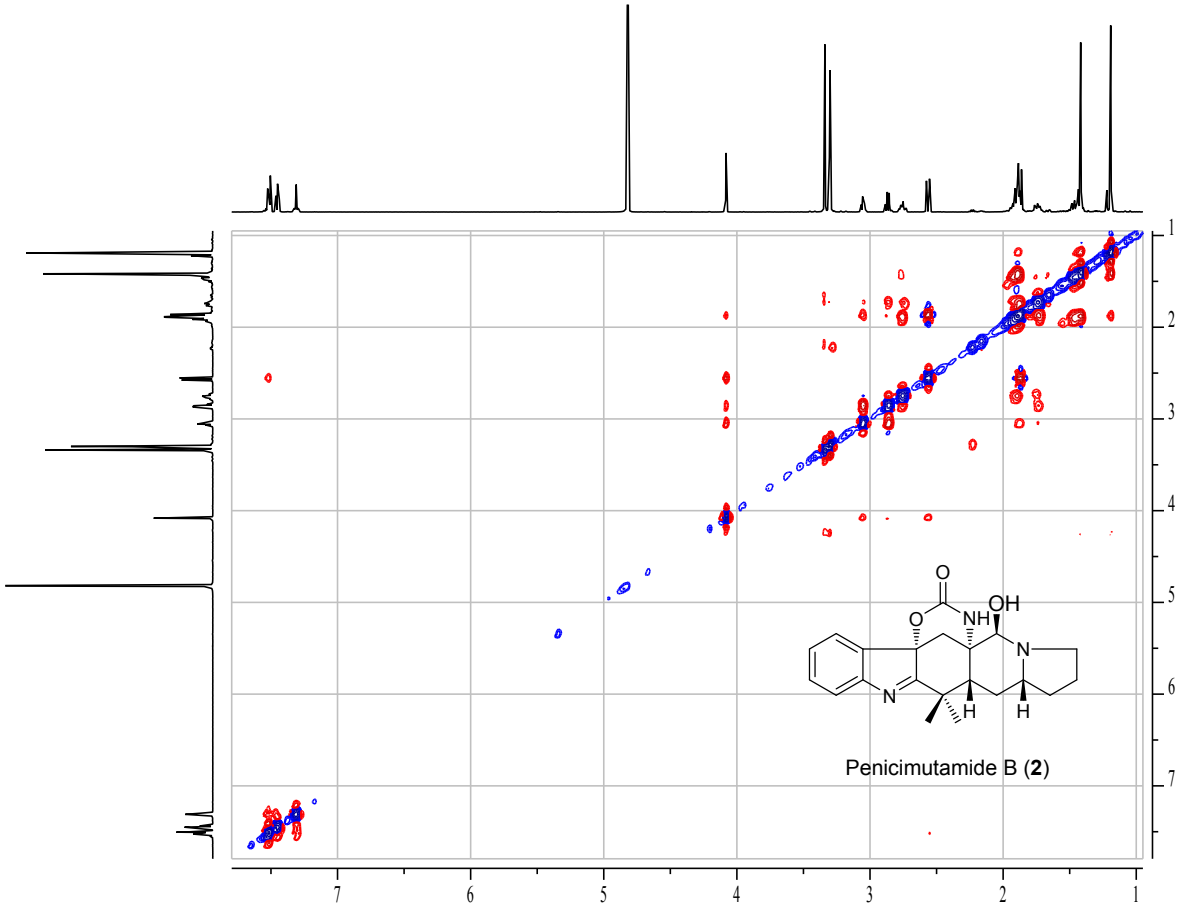
O
NH
OH
O
N
N
H
H
Penicimutamide B (2)
1
2
3
4
5
6
7
7
6
5
4
3
2
1

Figure S31. Positive and negative ion ESI-MS spectra of **3**.

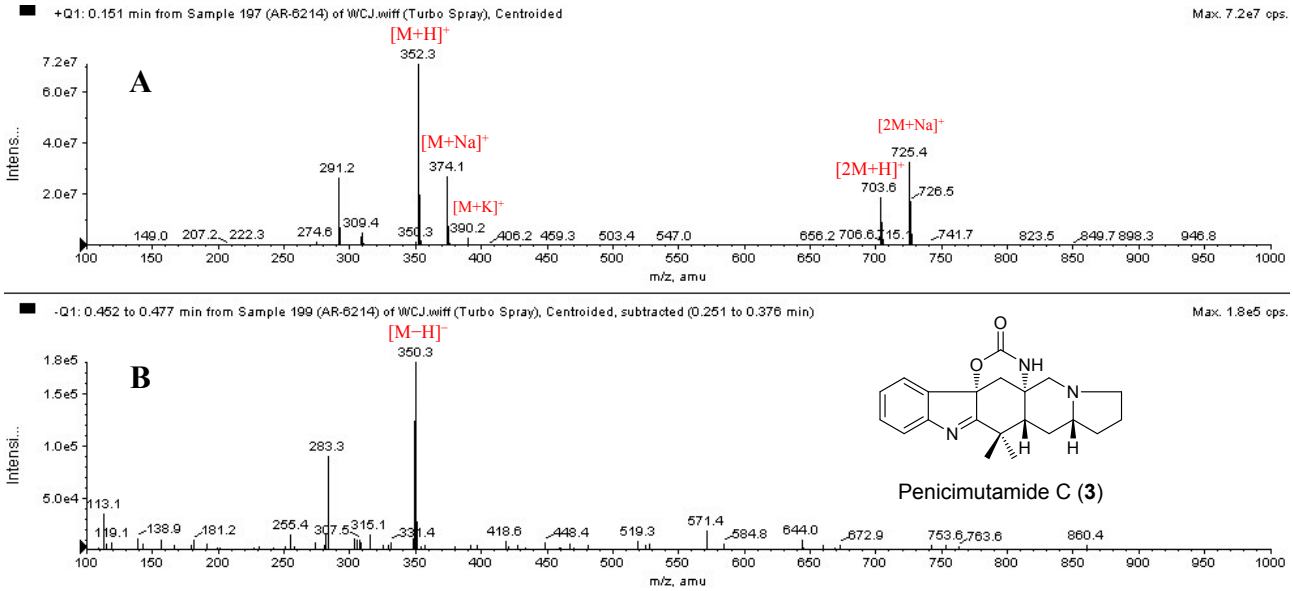

Figure S32. Positive ion HR-ESI-MS spectrum of **3**.

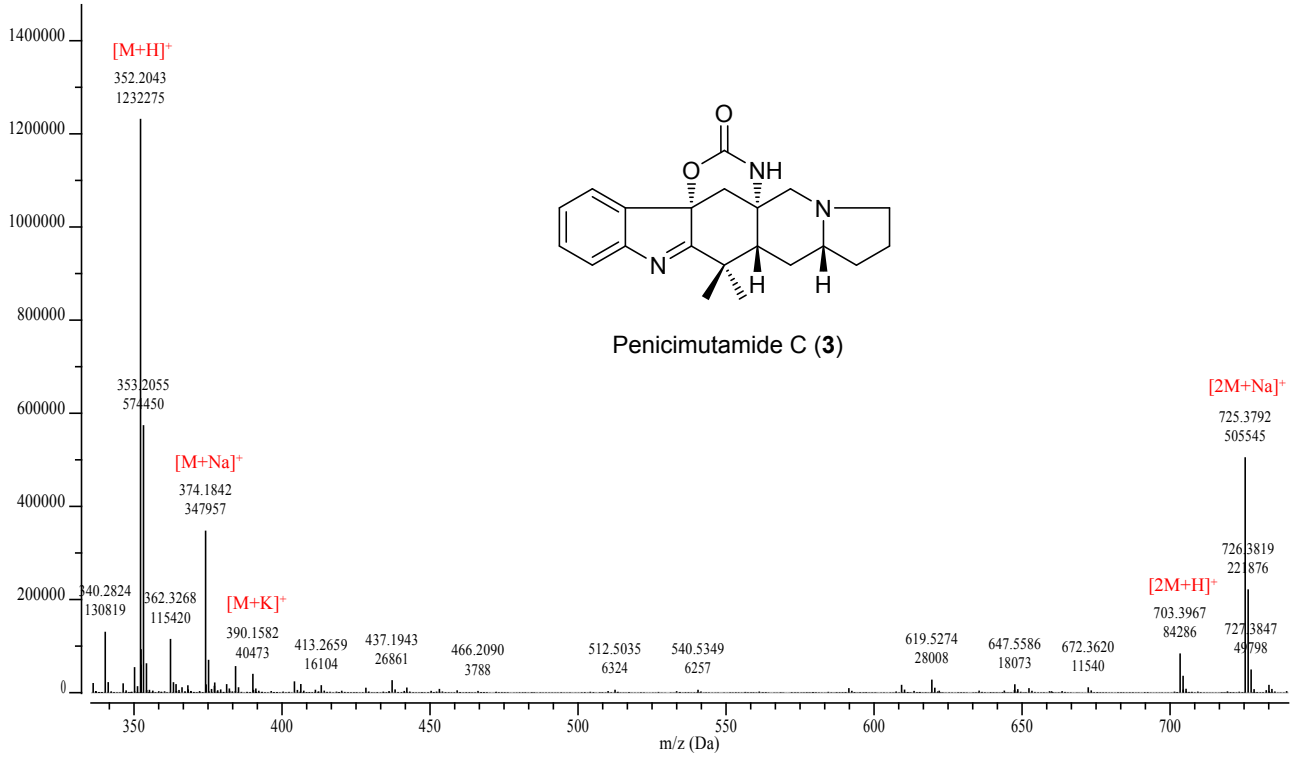

Figure S33. UV spectrum of **3** in MeOH.

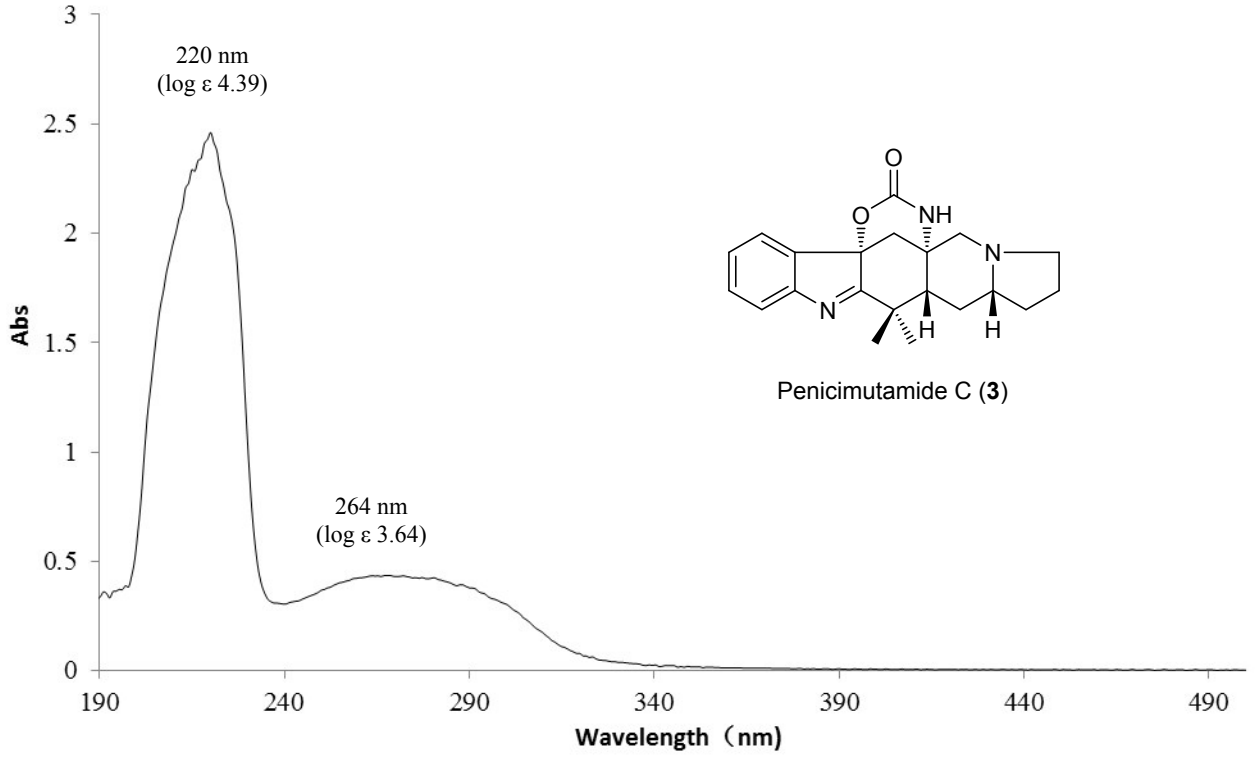

Figure S34. IR spectrum of **3** (measured on a diamond ATR crystal).

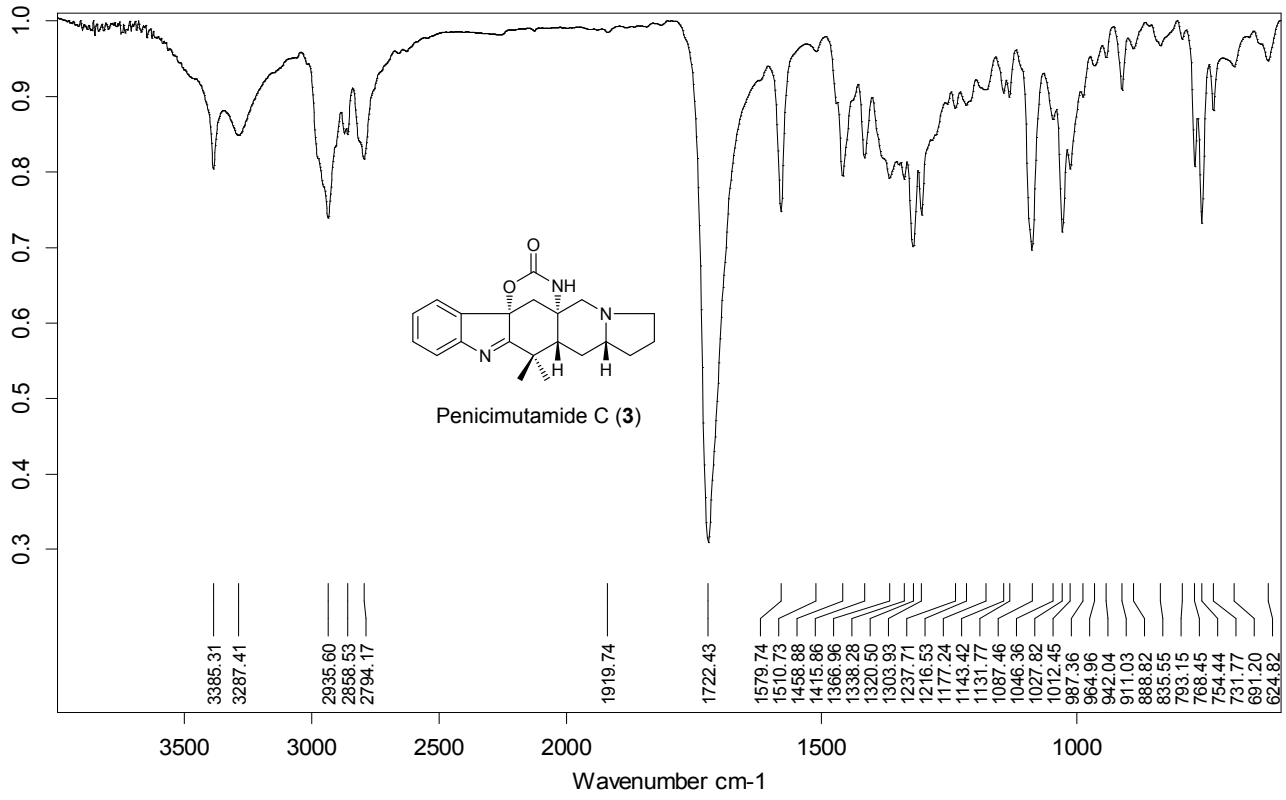

Figure S35. 600 MHz ^{1}H NMR spectrum of **3** in CD_3OD.

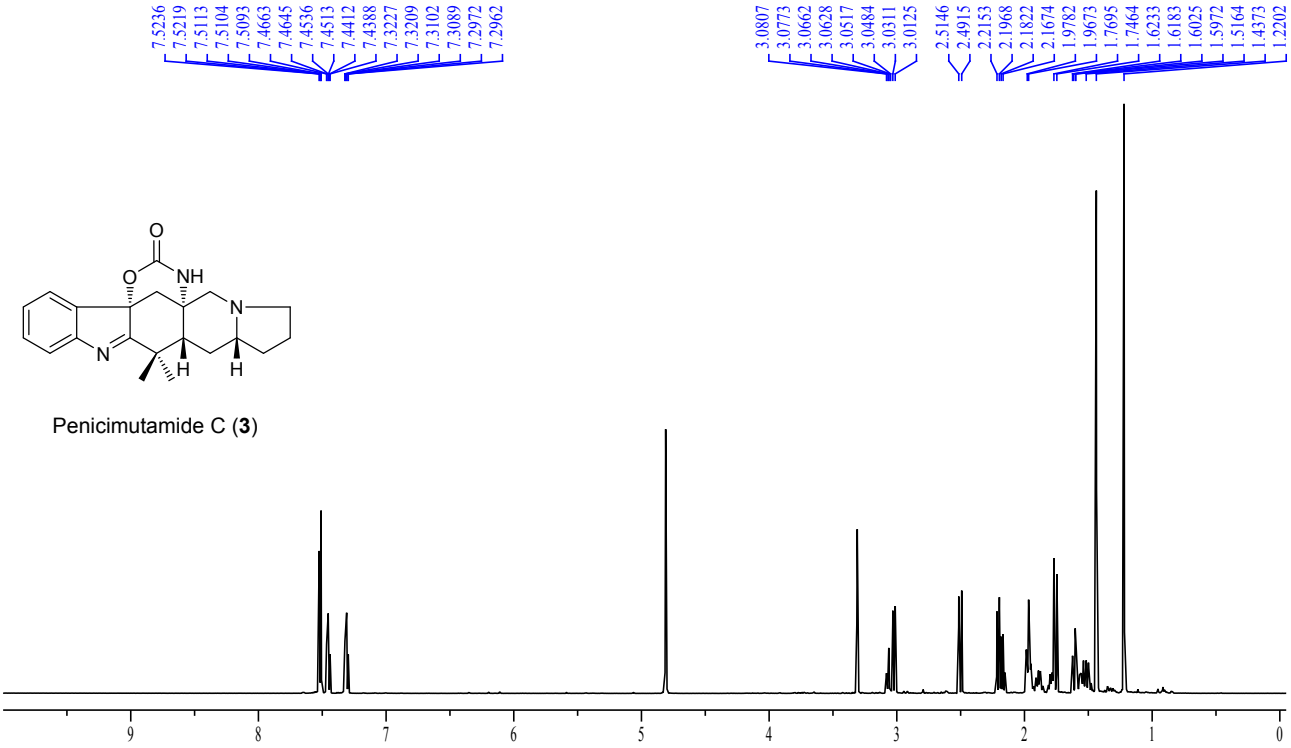

Figure S36. Enlarged 600 MHz ^{1}H NMR spectrum of **3** in CD_3OD.

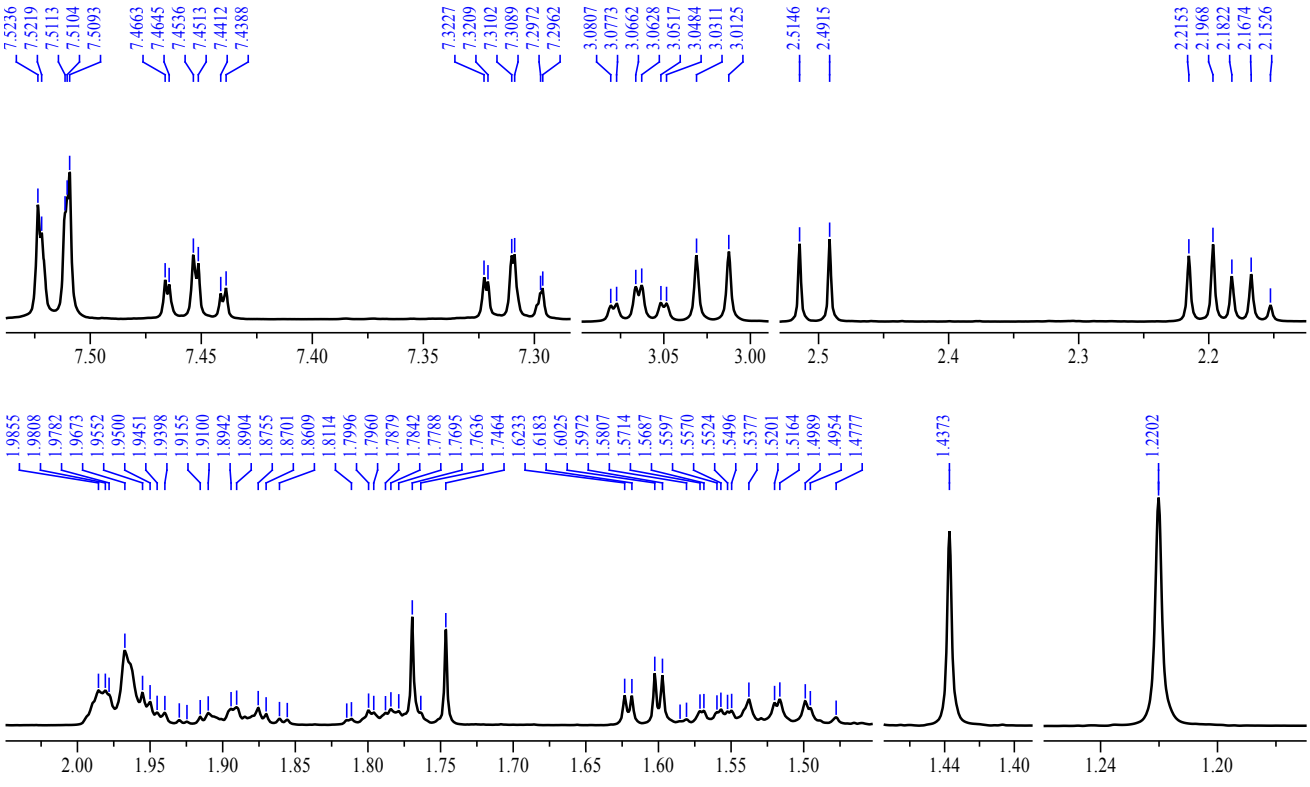

Figure S37. 150 MHz ^{13}C NMR spectrum of **3** in CD_3OD.

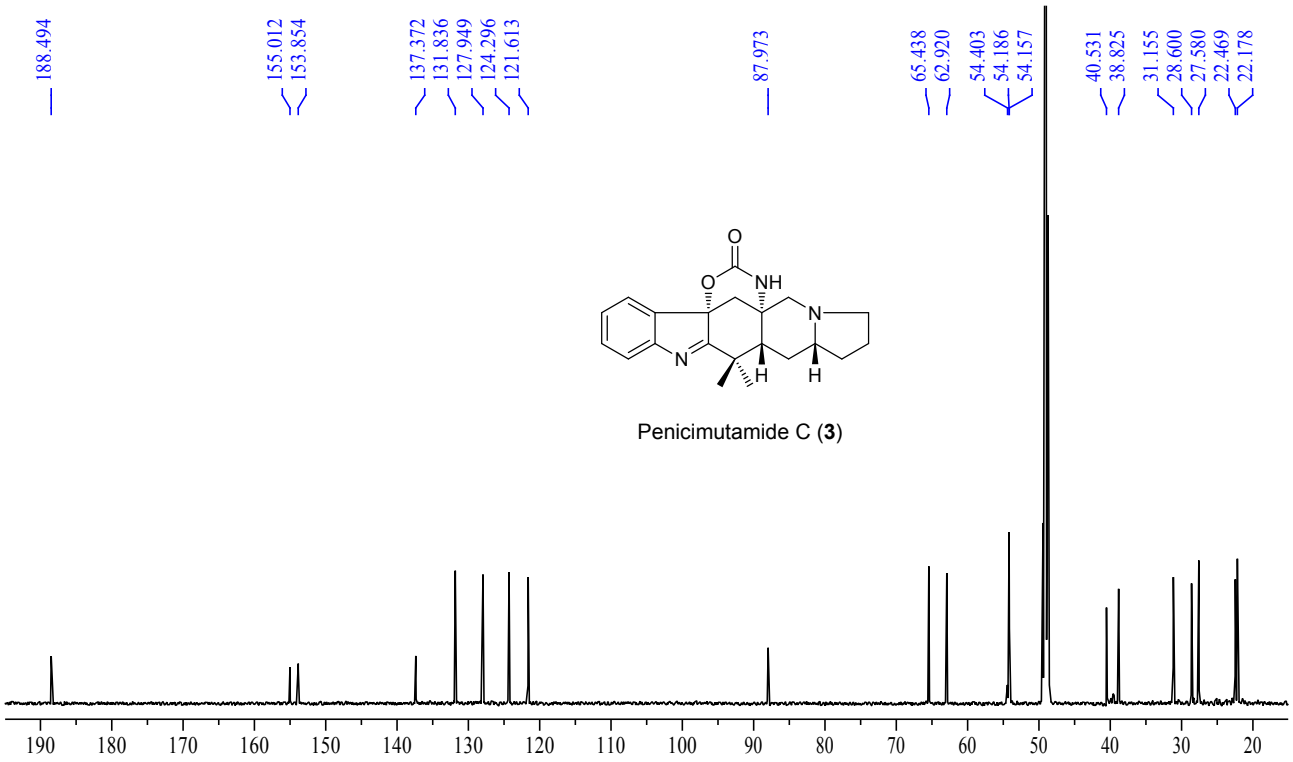

Figure S38. 150 MHz DEPT spectra of **3** in CD_3OD.

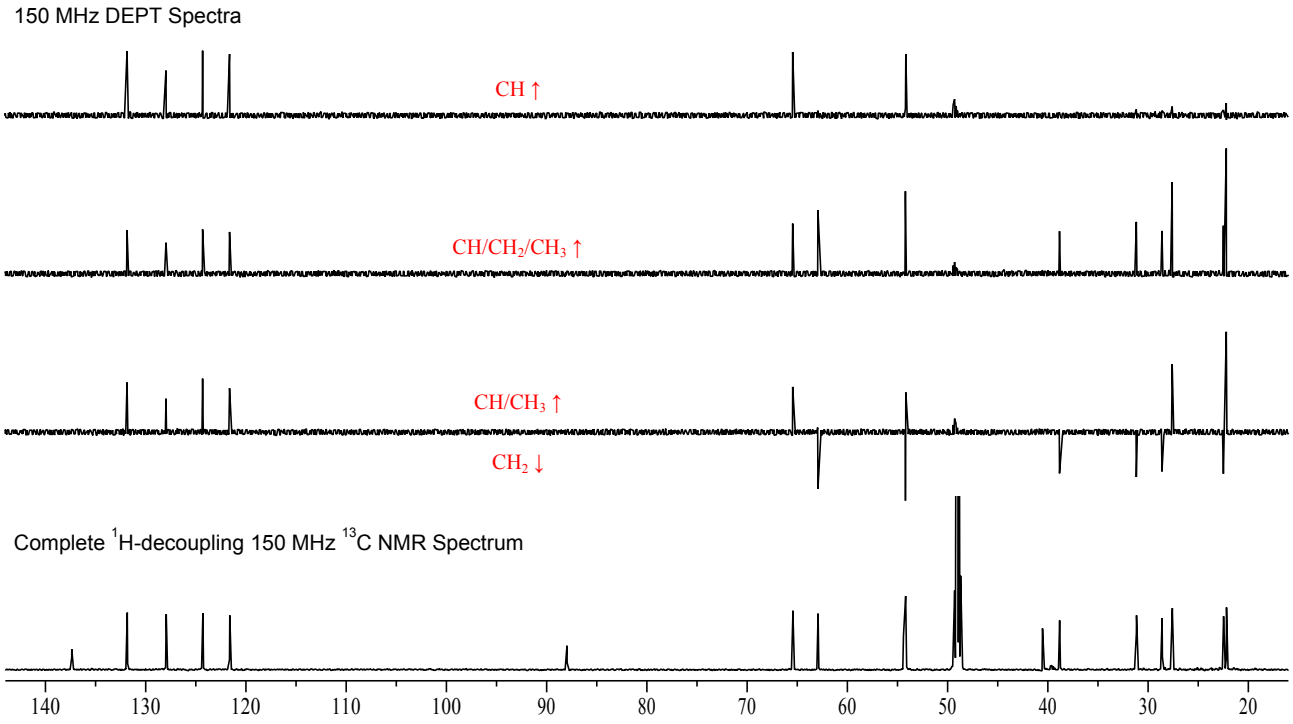

Figure S39. 600 MHz ^{1}H-^{1}H COSY spectrum of **3** in CD_3OD.

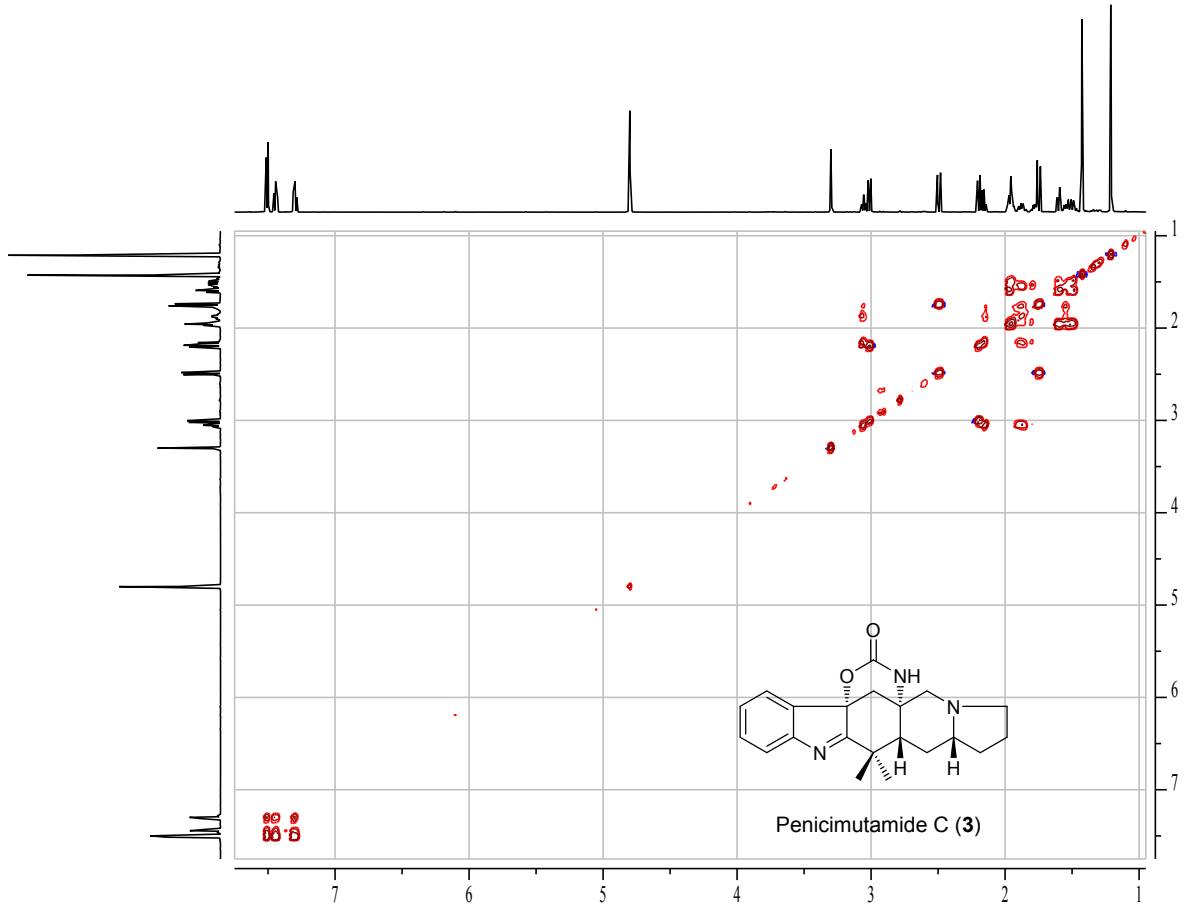

Figure S40. 600 MHz ^{1}H/150 MHz ^{13}C HMQC spectrum of **3** in CD_3OD.

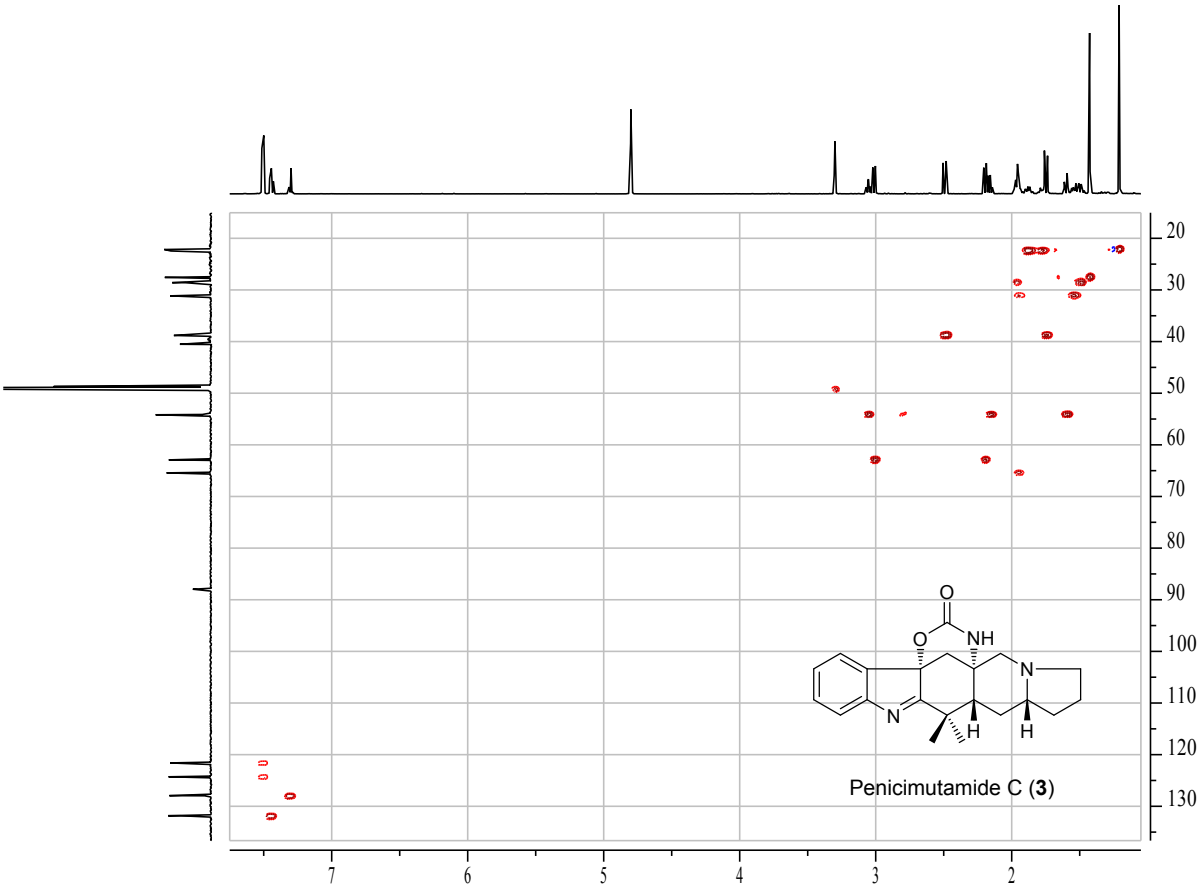

Figure S41. 600 MHz ^{1}H/150 MHz ^{13}C HMBC spectrum of **3** in CD_3OD.

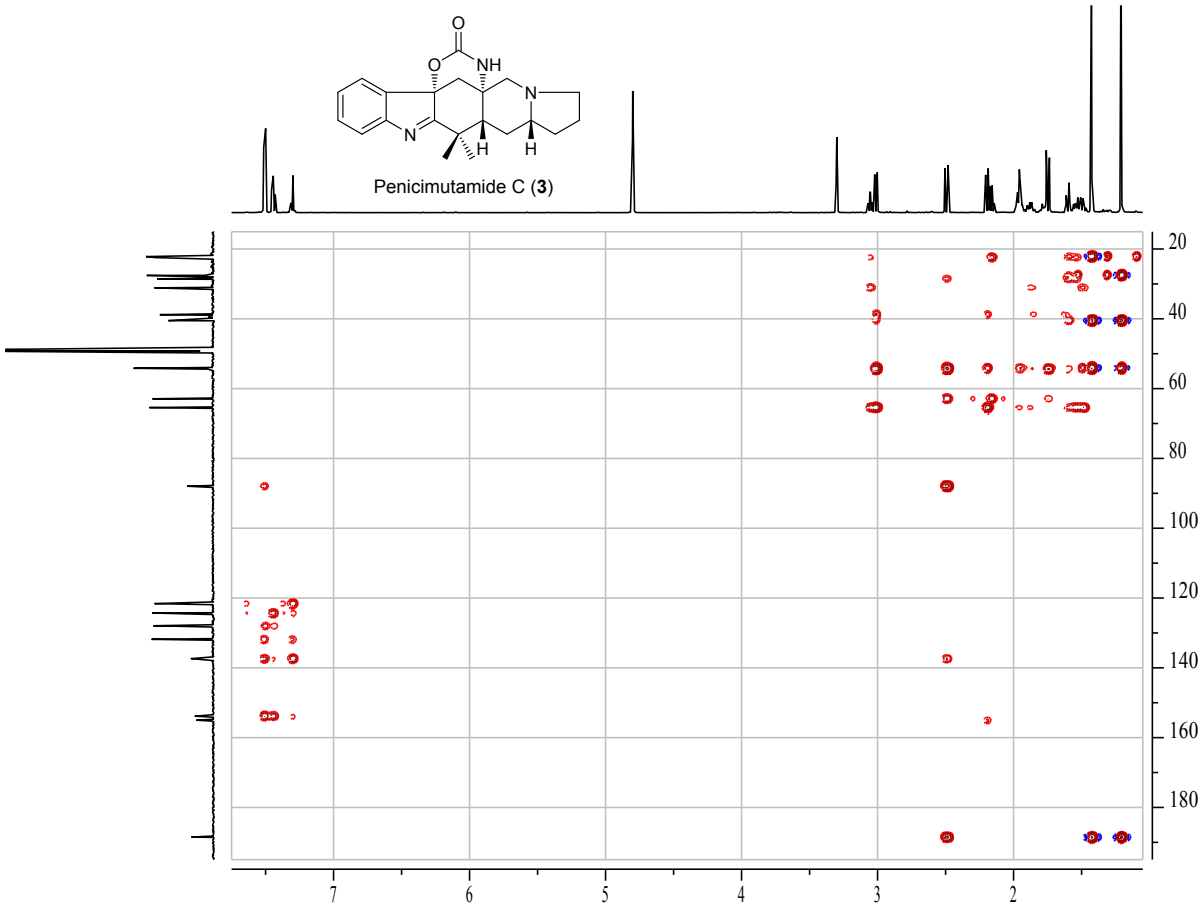

Figure S42. 600 MHz NOESY spectrum of **3** in CD_3OD.